

# A high-throughput microfluidic nano-immunoassay for detecting anti-SARS-CoV-2 antibodies in serum or ultra-low volume dried blood samples

Zoe Swank<sup>1</sup>, Grégoire Michielin<sup>1</sup>, Hon Ming Yip<sup>1</sup>, Patrick Cohen<sup>2</sup>, Diego O. Andrey<sup>2,3</sup>, Nicolas Vuilleumier<sup>2</sup>, Laurent Kaiser<sup>3,4,5</sup>, Isabella Eckerle<sup>\*†3,4,5</sup>, Benjamin Meyer<sup>\*‡6</sup>, and Sebastian J. Maerkl<sup>\*§1</sup>

<sup>1</sup> Institute of Bioengineering, School of Engineering, École Polytechnique Fédérale de Lausanne, Lausanne, Switzerland

<sup>2</sup>Division of Laboratory Medicine, Department of Diagnostics, Geneva University Hospitals and Geneva University, Geneva, Switzerland

<sup>3</sup>Division of Infectious Diseases, Department of Medicine, Geneva University Hospitals and Faculty of Medicine, Geneva, Switzerland

<sup>4</sup>Laboratory of Virology, Division of Laboratory Medicine, Geneva University Hospitals and Faculty of Medicine, Geneva, Switzerland

<sup>5</sup>Center for Emerging Viral Diseases, Geneva University Hospitals & Faculty of Medicine, Université de Genève, Geneva, Switzerland

<sup>6</sup>Centre for Vaccinology, Department of Pathology and Immunology, University of Geneva, Geneva, Switzerland

February 7, 2021

---

\* contributed equally

† Correspondence: [isabella.eckerle@hcuge.ch](mailto:isabella.eckerle@hcuge.ch)

‡ Correspondence: [benjamin.meyer@unige.ch](mailto:benjamin.meyer@unige.ch)

§ Correspondence: [sebastian.maerkl@epfl.ch](mailto:sebastian.maerkl@epfl.ch)

## Abstract

Novel technologies are needed to facilitate large-scale detection and quantification of severe acute respiratory syndrome coronavirus 2 (SARS-CoV-2) specific antibodies in human blood samples. Such technologies are essential to support seroprevalence studies, vaccine clinical trials, and to monitor quality and duration of immunity. We developed a microfluidic nano-immunoassay for the detection of anti-SARS-CoV-2 IgG antibodies in 1024 samples per device. The method achieved a specificity of 100% and a sensitivity of 98% based on the analysis of 289 human serum samples. To eliminate the need for venipuncture, we developed low-cost, ultra-low volume whole blood sampling methods based on two commercial devices and repurposed a blood glucose test strip. The glucose test strip permits the collection, shipment, and analysis of 0.6  $\mu$ L whole blood easily obtainable from a simple fingerprick. The nano-immunoassay platform achieves high-throughput, high sensitivity and specificity, negligible reagent consumption, and a decentralized and simple approach to blood sample collection. We expect this technology to be immediately applicable to current and future SARS-CoV-2 related serological studies and to protein biomarker diagnostics in general.

## 1 **Introduction**

2 The emergence of a new coronavirus at the end of 2019, termed severe acute respiratory syndrome coro-  
3 navirus 2 (SARS-CoV-2), led to an unprecedented global public health crisis [1]. Over a year later, it is  
4 estimated that SARS-CoV-2 infected over 100 million people worldwide and two million people died of  
5 coronavirus disease 2019 (COVID-19) caused by SARS-CoV-2 [2]. As SARS-CoV-2 causes mainly mild  
6 disease or infection presents without symptoms, many cases are not captured by direct testing in the acute  
7 phase of disease [3]. However, to estimate infection fatality rate and guide public health decisions, it is of  
8 utmost importance to establish the true spread or prevalence of the virus by identifying how many people  
9 have been exposed [4, 5].

10 Detection of anti-SARS-CoV-2 antibodies using highly sensitive and specific assays can help answer  
11 these questions. Several seroprevalence studies have already been conducted, demonstrating rather low  
12 seroprevalence rates even in areas that were severely affected [6, 7, 8, 9]. Such data show that herd immunity  
13 through natural infection is far from being reached. However, these studies are merely snapshots of an  
14 evolving situation, both in time and space. Therefore, there is a sustained need for seroprevalence studies to  
15 be continuously conducted in order to monitor virus spread and to keep policy makers informed. In addition,  
16 tens to hundreds of thousands of blood samples will need to be tested to determine antibody titers for each  
17 SARS-CoV-2 vaccine phase 3 clinical trial and a large number of samples will need to be tested to monitor  
18 immune responses after a vaccine has been approved and rolled-out. Such studies are cumbersome and  
19 expensive to perform as they require large-numbers of serum samples to be obtained by venipuncture and  
20 analysed by highly sensitive and specific immunological assays to classify samples or to provide quantitative  
21 information on antibody titers.

22 Several assays, such as enzyme-linked immunosorbent assays (ELISA) or chemiluminescent immuno-  
23 assays (CLIA), are commercially available, but mainly rely on serum drawn by venipuncture. These tests  
24 are also rather expensive, with reagent costs on the order of 3-10 USD per test. Alternatively, in-house  
25 ELISAs are difficult to standardize and require high amounts of recombinant antigen, usually around 100ng  
26 per sample [5]. Other recently developed methods such as miniaturized high-throughput ELISAs that use  
27 low microliter volumes suffer from lower sensitivity [10], and ultra-sensitive assays based on digital ELISA  
28 have a low sample throughput of 68 tests per hour [11]. The comparatively high cost of these assays and the  
29 reliance on serum samples taken by venipuncture are considerable hurdles to performing large-scale studies  
30 under normal circumstances, but especially so during a pandemic, when sample collection can put clinical

31 staff and study participants at risk. Lateral flow assays (LFAs) can be performed at the point of care or at  
32 home requiring only a "drop" of whole blood, but the sensitivity and specificity of these assays is often  
33 insufficient [12, 13, 14] and LFAs are relatively expensive at ~22 USD per test. Furthermore, LFAs provide  
34 test results but no blood samples are being collected which could be used for follow-up analyses.

35 There is therefore a clear need for new technologies to supersede existing methods such as ELISA,  
36 CLIA, and LFAs. Novel technologies should be capable of high-throughput, low-reagent consumption, low-  
37 cost per test, high sensitivity and specificity, and be compatible with ultra-low volume whole-blood samples  
38 in the low or even sub-microliter range that can be obtained via a simple fingerprick. Biomarker detection  
39 using dried whole blood on filter paper or other devices would have tremendous advantages as it can be  
40 collected by untrained individuals at home. The samples could then be conveniently shipped by regular  
41 mail at ambient temperature to a central laboratory for analysis and test results returned electronically via a  
42 mobile app or email.

43 In this study we developed and validated a nano-immunoassay (NIA) that analyses 1024 samples in  
44 parallel on a single microfluidic device the size of a USB stick. NIA reagent consumption and corresponding  
45 costs are roughly 1000 times less than a standard ELISA. Based on the analysis of 134 negative and 155  
46 positive control sera, NIA achieved a specificity of 100% and a sensitivity of 98% when RT-PCR was used  
47 as a reference. NIA performed as well as a standard ELISA for samples obtained more than 20 days post  
48 onset of symptoms, and performed better than ELISA for samples obtained less than 20 days past onset of  
49 symptoms, indicating that NIA is more sensitive than ELISA for the analysis of early timepoint samples  
50 with lower antibody titers. We go on to demonstrate that NIA can be used to measure anti-SARS-CoV-2  
51 antibodies in ultra-low volume dried whole blood samples, eliminating the need for venipuncture blood  
52 collection. We tested two commercial blood collection devices: Neoteryx's Mitra<sup>®</sup> and DBS System SA's  
53 HemaXis<sup>™</sup> DB10, and show that it is possible to repurpose low-cost and widely available blood glucose  
54 test strips for sample collection and shipment. Samples could be stored up to 6 days at room temperature  
55 with minimal sample degradation and all three methods yielded better results than an ELISA performed on  
56 standard serum samples collected from the same individuals.

## 57 **Results**

### 58 **Nano-immunoassay development**

59 We adapted a MITOMI based [15, 16] 1024 NIA device previously applied to vaccine adjuvant screening  
60 [17] and the detection of inflammatory and cancer related protein biomarkers in serum [18] to the detection  
61 of anti-SARS-CoV-2 IgG antibodies. The NIA device described here is a simplified version of the original  
62 1024 serum analyzer chip and more similar to the original MITOMI device with slightly enlarged chambers  
63 to accommodate spotted patient samples. The microfluidic device is a standard two-layer polydimethylsilox-  
64 ane (PDMS) device [19], consisting of a flow and a control layer. Fluids in the flow layer can be manipulated  
65 with pneumatic valves formed by the control layer. The device contains 1024 unit cells, each consisting of  
66 an assay and a spotting chamber (Figure 1A). Patient samples are spotted onto an epoxy-coated glass slide  
67 using a contact-printing microarray robot, on top of which the PDMS device is aligned and bonded. Patient  
68 samples are initially isolated by actuating the neck valve and the surface of the assay chamber is patterned  
69 with biotinylated bovine serum albumin (BSA-biotin) and neutrAvidin, leaving a circular surface region  
70 coated with neutrAvidin beneath the MITOMI button. Afterwards, biotinylated anti-His antibody is flowed  
71 through the device, enabling the subsequent immobilization of a His-tagged SARS-CoV-2 antigen. Patient  
72 samples are then solubilized and the sandwich valves are closed, allowing any SARS-CoV-2 specific anti-  
73 bodies to diffuse into the assay chamber and bind the surface immobilized antigen. The MITOMI button  
74 is closed following an incubation period and any unbound material is washed away. A secondary antibody  
75 labeled with phycoerythrin (PE) is flowed to detect the presence of antibodies bound to the SARS-CoV-2  
76 antigen (Fig. 1B, C).

77 We optimized the NIA for detection of anti-spike IgG antibodies in human serum by first testing sev-  
78 eral different spike antigen variants and identified the in-house produced trimerized full-length spike protein  
79 as the most suitable antigen (Fig. S1). The use of trimerized full length spike and spike-receptor binding  
80 domain (RBD) both resulted in high signal intensities and low-background. We decided on using the trimer-  
81 ized full-length spike protein as it most closely resembles the natural conformation of the SARS-CoV-2  
82 spike protein. As a proof-of-concept we added chimeric anti-spike antibody at different concentrations into  
83 human serum, spotted each dilution, and showed that NIA could quantify anti-spike antibody concentra-  
84 tions (Fig. 1D, E). Based on this sandwich immunoassay we estimate that our limit of detection (LOD) is  
85 around 1 nM IgG. To permit the analysis of patient sera in a standard, biosafety level 1 (BSL-1) laboratory  
86 we developed a simple treatment protocol that renders the sera BSL-1 compatible. This was achieved by

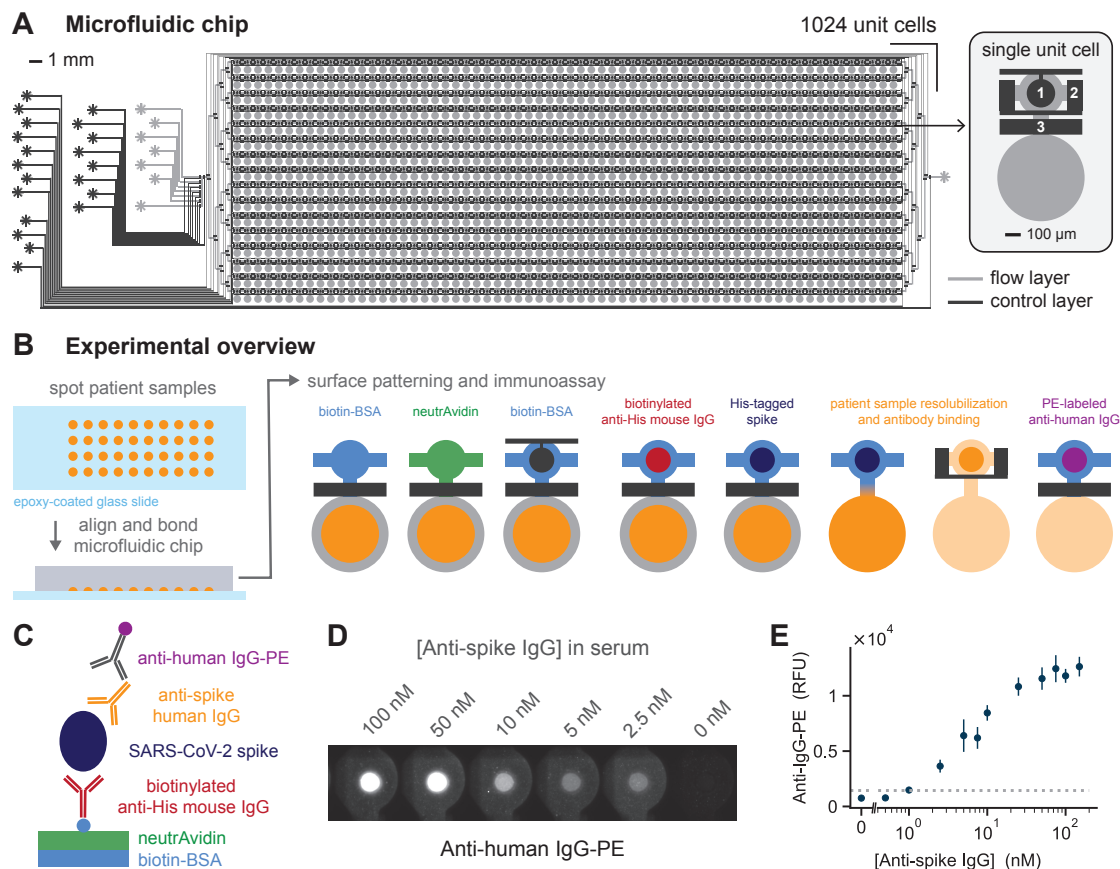


Figure 1: **High-throughput microfluidic nano-immunoassay for anti-SARS-CoV-2 antibody detection.**

(A) The two-layer microfluidic chip design consists of 1024 unit cells. Each unit cell in turn contains two sections: an immunoassay chamber (top) and a spotting chamber (bottom). Control valves include the button (1), sandwich (2) and neck (3) valves. (B) A schematic of the experimental process, starting with the spotting of patient samples, followed by chip alignment and bonding, biotin-BSA and neutrAvidin surface patterning, and lastly the immunoassay for detection of anti-SARS-CoV2 antibodies. Surface patterning and immunoassay are shown for a single unit. During the experiment all unit cells are processed in parallel. (C) Schematic of the on-chip sandwich immunoassay. (D) Fluorescence images of anti-human IgG-PE signal for a given concentration of anti-spike antibodies present in human serum. (E) Quantification of the anti-human IgG-PE signal for a range of anti-spike concentrations spotted. The dashed horizontal line indicates the LOD.

87 conducting a short heat-inactivation step, followed by the addition of Triton X-100 to a final concentration  
88 of 1% [20]. Dried whole blood samples could be safely handled in a BSL-1 environment without requiring  
89 any pre-treatment steps.

## 90 **Nano-immunoassay validation**

91 We validated the high-throughput NIA for the detection of SARS-CoV-2 anti-spike IgG antibodies with  
92 289 serum samples, collected from 155 PCR-confirmed SARS-CoV-2 infected individuals and 134 pre-  
93 pandemic negative samples collected in 2013/14 and 2018. Different serum sample dilutions, ranging from  
94 no dilution to a 1:256 dilution, were spotted to determine the optimal value (Fig. S2). NIA achieved a  
95 maximum specificity and sensitivity of 100% and 98%, respectively, at a serum dilution of 1:8 (Fig. 2A,  
96 S2) and a receiver operator characteristic (ROC) curve with an area under the curve (AUC) equal to 0.99  
97 (Fig. 2B). In parallel, ELISA was used to validate the presence of anti-spike(S1) IgG in the same patient  
98 samples (Fig. 2C) resulting in a good correlation ( $R^2=0.87$ ) between NIA and ELISA measurements (Fig.  
99 2D). As the serum samples were obtained from patients at different time points post onset of symptoms  
100 we plotted the NIA results according to when samples were obtained (Fig. 2E). We also analyzed NIA and  
101 ELISA results split into samples obtained on or before 20 days post onset of symptoms (DPOS) and samples  
102 obtained after 20 days post onset when antibody responses are usually fully developed (Fig. 2A, C). If DPOS  
103 was not known for a given patient, then days post diagnosis (DPD) was used instead. Performance in terms  
104 of specificity and sensitivity between NIA and ELISA are similar for samples obtained after 20 days past  
105 onset of symptoms, but NIA outperforms ELISA for samples collected on or before 20 days post onset in  
106 terms of sensitivity by 13 percentage points (Fig. 2F). In addition, four other commercially available assays  
107 were used to detect anti-SARS-CoV-2 IgG antibodies present in a subset of the COVID-19 patient serum  
108 samples. For samples collected after 20 days post onset NIA performed as well as 2 other commercial  
109 assays and outperformed 2 of these assays in terms of sensitivity. Furthermore, NIA outperformed all 5  
110 commercially available assays in terms of sensitivity for samples collected less than 20 days post onset by  
111 at least 9 percentage points or more (Fig. S3).

112 Each sample dilution was tested in triplicate, enabling us to test up to 336 different samples or sample  
113 dilutions on a single device. In order to determine if it would be possible to further increase throughput by  
114 reducing the number of replicates we randomly selected one or two of the three 1:8 dilution replicates and  
115 calculated ROC curves, specificity, and sensitivity (Fig. S4). We found that using duplicates only slightly  
116 reduced sensitivity from 98% to 97%, whereas using a single measurement lowered sensitivity to 95%, all

117 the while retaining a 100% specificity. Given that using duplicate measurements led to only a minimal  
118 change in sensitivity, it will be possible to increase throughput to 512 samples analyzed in duplicate per  
119 device. Additional gains in throughput are theoretically possible by scaling the device itself, with MITOMI  
120 devices containing up to 4160 unit cells having been demonstrated in the past [21].

121 To assess device to device reproducibility we tested all serum samples (1:8 dilution) on two separate  
122 devices which resulted in a correlation of  $R^2 = 0.98$  (Fig. S5A). We then correlated the measurements from  
123 one of those devices to the measurements made on six other devices and again observed a good correlation of  
124  $R^2 = 0.95$  (Fig. S5B). In the first case the same sample solution was used for spotting two devices, whereas  
125 in the second case the two measurements being compared came from separately prepared patient sample  
126 dilutions. Additionally we compared the anti-IgG-PE signal measured for a reference serum dilution series  
127 on three separate devices and computed an average coefficient of variation equal to 11.7% for the dilutions  
128 measured (Fig. S5C, D).

129 To determine quantitative antibody titers in each serum sample, we fit data from the full dilution series to  
130 a saturation binding curve model, enabling us to extract the dilution equivalent to the half-maximum signal  
131 for each serum sample ( $EC_{50}$ ) (Fig. 2G, S6). Using the calculated  $1/EC_{50}$  value, we again analyzed the NIA  
132 results, resulting in a specificity and sensitivity of 100% and 98%, respectively (2H). Lastly, we compared  
133 the  $1/EC_{50}$  values to values obtained from a single 1:8 dilution and found an excellent correspondence be-  
134 tween those two measurements (Fig. 2I), indicating that a single measurement returns accurate quantitative  
135 information on antibody concentrations. Only at very high antibody titers does the signal saturate for the  
136 1:8 dilution. Using two measurements of a 1:8 and one slightly higher dilution could therefore maximize  
137 throughput, specificity, and sensitivity of NIA, and return accurate antibody titer values.

## 138 **Ultra-low volume whole blood collection and analysis**

139 The NIA platform proved to be highly specific and sensitive when applied to standard serum samples. We  
140 recognized that use of serum samples limits the applicability of our and other methods to samples collected  
141 by venipuncture, which has to be performed by trained personnel in hospitals or point of care settings.  
142 Venipuncture requires large volumes of blood in the 5 mL range, considerable downstream sample process-  
143 ing, and a cold chain from point of sample collection to point of analysis. Large-scale seroprevalence studies  
144 are thus challenging to conduct, especially when including remote or large geographic areas. Establishing a  
145 large-scale, low-cost, and widely accessible serology platform necessitates the development of venipuncture  
146 alternatives. For this reason, we developed a sample collection and processing pipeline that enables us to



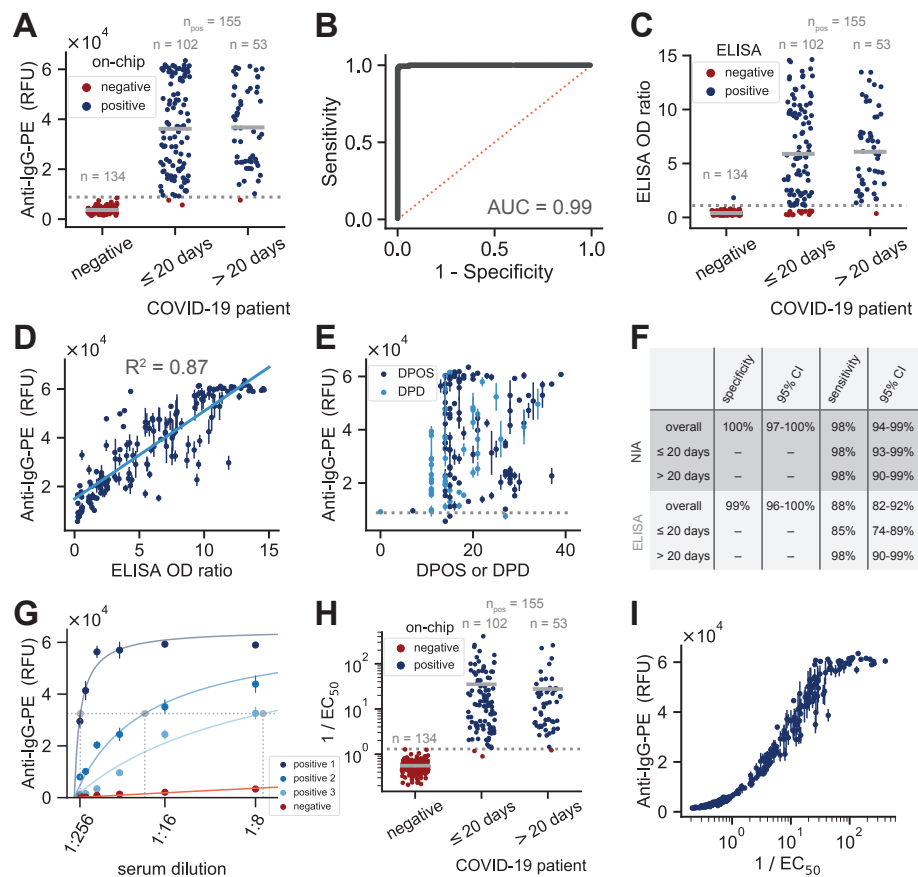


**Figure 2: Nano-immunoassay validation.** (A) NIA anti-IgG-PE signal for serum samples obtained from SARS-CoV-2 negative individuals (obtained in 2013/14 and 2018) or SARS-CoV-2 RT-PCR confirmed positive patients. Measurements shown are for a 1:8 dilution of each serum sample. Data points represent mean values of 3 replicates from a single chip. A total of 6 devices were run to collect this data. (B) ROC curve corresponding to the measurements shown in panel A. (C) ELISA OD ratios for the same serum samples as in A. (D) Correlation between NIA and ELISA measurements. Data points represent means  $\pm$  SD ( $n = 3$ ). (E) NIA measurements plotted versus days past onset of symptoms or days post diagnosis. Data points represent means  $\pm$  SD ( $n = 3$ ). (F) Specificity and sensitivity for NIA and ELISA. The dashed grey lines in A, C, and E indicate the cutoff used for the specificity and sensitivity calculations. (G) Examples of curve fits for three positive and one negative patient sample. The horizontal dashed line indicates half maximal binding and the three dashed vertical lines correspond to the  $EC_{50}$  values determined for each of the positive samples. (H)  $1/EC_{50}$  categorized according to whether the sample was negative or from an RT-PCR confirmed positive patient. (I) Anti-IgG-PE signal for a 1:8 dilution of each serum sample versus  $1/EC_{50}$ .

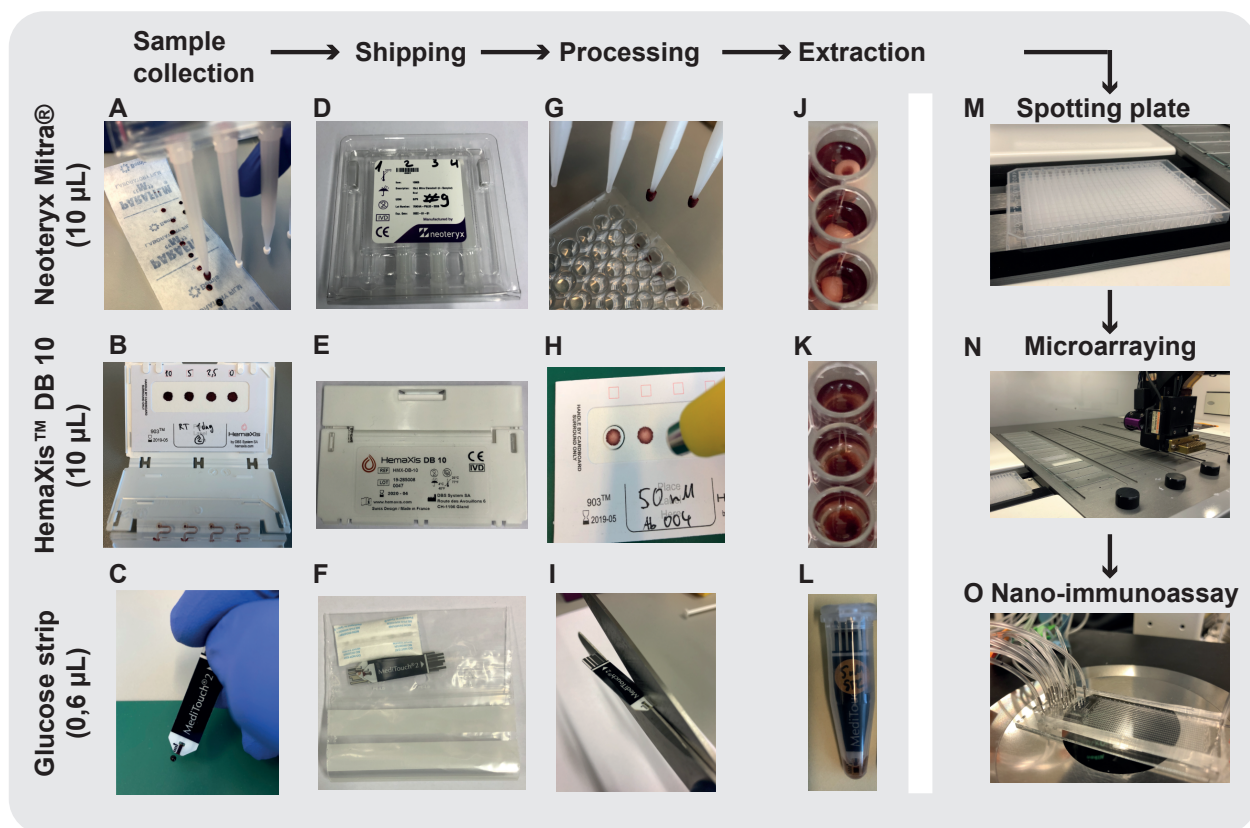


Figure 3: **Ultra-low volume whole blood sampling and processing.** Three devices were tested for ultra-low volume whole blood sampling and extraction: Neoteryx Mitra®, DBS System SA HemaXis™ DB10, and glucose test strips. 10 µL whole blood is collected by the (A) Mitra®d and (B) HemaXis™ DB10 devices. (C) 0.6 µL whole blood is collected by the blood glucose test strip. (D-F) Blood samples are dried, allowing the devices to be shipped under ambient conditions by regular mail. (G-I) The devices are processed upon arrival at the laboratory. (G) Mitra® tips are removed and placed in a 96 well plate, (H) HemaXis™ DB10 cards are punched and the filter discs placed in a 96 well plate, (I) and the glucose test strip is cut to size and placed in an Eppendorf tube. (J-L) Blood samples are extracted in a buffer solution by overnight incubation at 4°C, followed by transfer to a spotting plate (M). Samples are then microarrayed (N), and analyzed with the NIA device (O).

147 carry out NIA with ultra-low volume, dried whole blood samples obtainable by a simple fingerprick. We  
148 tested three different methods to collect, ship, process, extract, and analyze dried whole blood samples (Fig.  
149 3). We tested two commercially available devices that collect 10  $\mu\text{L}$  of whole blood: Neoteryx Mitra<sup>®</sup> and  
150 DBS System SA HemaXis<sup>™</sup> DB10. We also explored the possibility of repurposing existing blood glucose  
151 test strips (Medisana, MediTouch 2) for whole blood collection and shipping. The glucose test strips collect  
152 0.6  $\mu\text{L}$  of whole blood which is approximately twenty times less than what is required by the commercial  
153 devices and 10,000 times less blood than obtained by venipuncture. Furthermore, blood glucose test strips  
154 are cheap at less than 0.5 USD per strip and widely available, potentially avoiding any supply bottlenecks  
155 during a pandemic. The two commercial devices by comparison cost 5-10 USD or 1.25 - 2.5 USD per  
156 sample.

157 We evaluated the three collection methods by spiking human whole blood with different concentrations  
158 of anti-spike IgG and collected the blood with each collection device. We then extracted the dried blood  
159 from each device and spotted the samples for NIA analysis. We first tested an aqueous ethylenediaminete-  
160 traacetic acid (EDTA) solution and sonication for extraction [22], but the use of this buffer resulted in large  
161 and inconsistent spots during microarraying. We then tested PBS (phosphate-buffered saline, 1% BSA) or  
162 PBS (1% BSA, 0.5% Tween-20) [23] extraction buffers with overnight incubation at 4°C and found that  
163 the addition of 0.5% Tween-20 greatly improved the assay (data not shown). With this optimized sample  
164 extraction workflow we were able to quantitate anti-spike IgG from the dried blood samples (Fig. 4A-C,  
165 S7).

166 To assess the variability of each sampling method we collected whole blood spiked with anti-spike IgG  
167 three separate times and compared the on-chip antibody signal (Fig. S8A-C). We calculated the coefficient  
168 of variation for the technical repeats for each anti-spike concentration tested and found that it did not ex-  
169 ceed 15% for any of the three collection methods with an average CV of 5.7%, 7.7%, 9.2% for Mitra<sup>®</sup>,  
170 HemaXis<sup>™</sup> DB10, and the glucose test strips (Fig. S8D). Although, there may be further variability intro-  
171 duced depending on how each individual collects his or her own blood sample, each device uses a hard-coded  
172 method to collect a specific volume of blood that leads to low variability for NIA antibody detection.

173 As we expect these blood sampling devices to be used decentralized, followed by shipping with regular  
174 mail to a central laboratory for analysis, an important factor to assess was sample stability. To determine  
175 stability of anti-spike IgG antibodies we allowed the blood to dry on each device followed by storage for two  
176 and six days at room temperature (23°C) before extraction and testing (Fig. 4D-F). Furthermore, depending  
177 on the climatic conditions, samples sent by post may be subject to higher temperatures, therefore we also

178 stored the devices for 1 day at 55°C. For the Mitra<sup>®</sup> device we observed very little sample degradation  
 179 after 6 days of storage at room temperature and slight sample degradation when stored at 55°C for one  
 180 day. Very similar results were obtained for the glucose test strips. The HemaXis<sup>™</sup>DB10 devices were the  
 181 most sensitive to prolonged and high temperature storage, but still resulted in sufficient signal for accurate  
 182 quantitation.

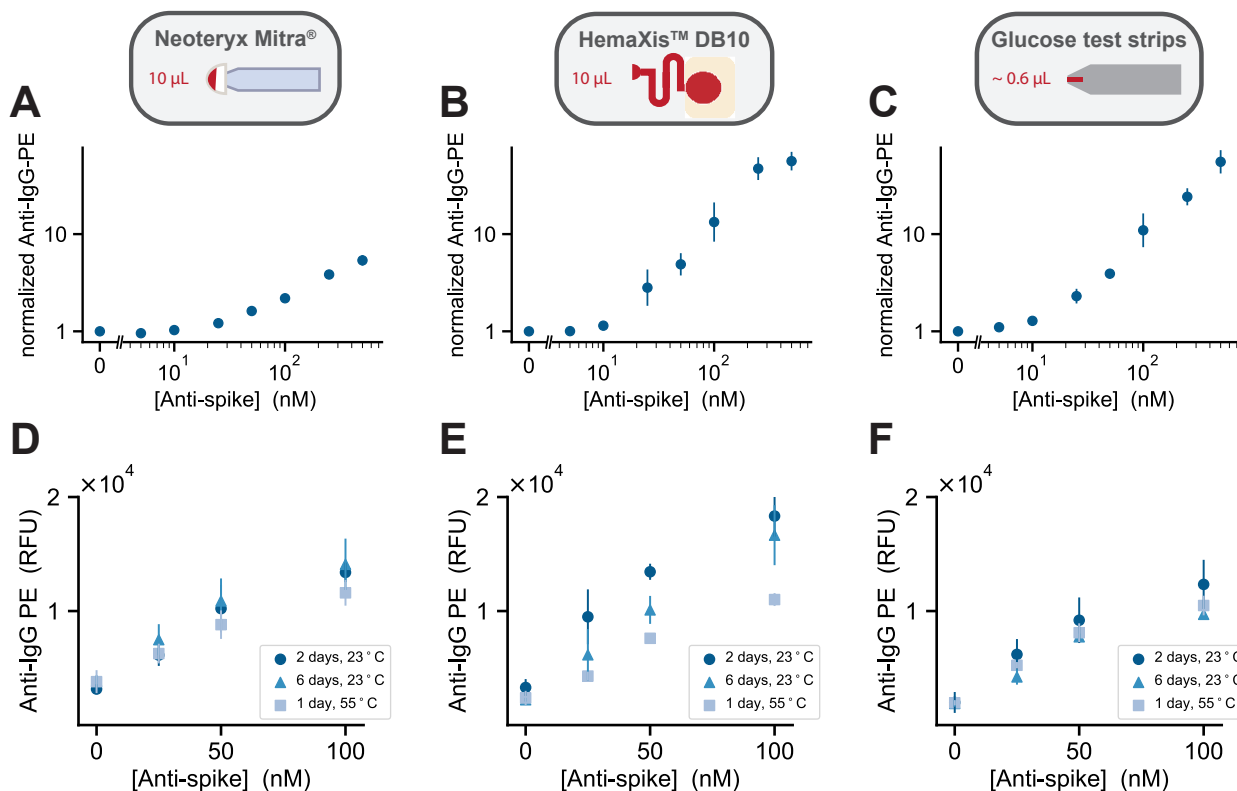


Figure 4: **Ultra-low volume dried blood method characterization.** The figure is organized into three columns each corresponding to the respective sampling method: Neoteryx Mitra<sup>®</sup>, HemaXis<sup>™</sup> DB10, and glucose test strips. (A-C) Normalized NIA anti-IgG-PE signal versus concentration of anti-spike IgG present in dried whole blood samples collected with each of the three sampling methods. Data points represent means  $\pm$ SD (n=4). The normalized signal is calculated by dividing the mean value for a given anti-spike concentration by the negative control mean value for 0 nM anti-spike. (D-F) Sample stability testing. NIA anti-IgG-PE measurements versus anti-spike IgG concentration. Blood samples were dried and then stored on each collection device for 1 day or 6 days at 23°C, and 1 day at 55°C.

183 Having established that ultra-low volume dried blood samples can be analyzed on the NIA platform,  
 184 we tested the method with ultra-low volume whole blood patient samples collected with each of the three

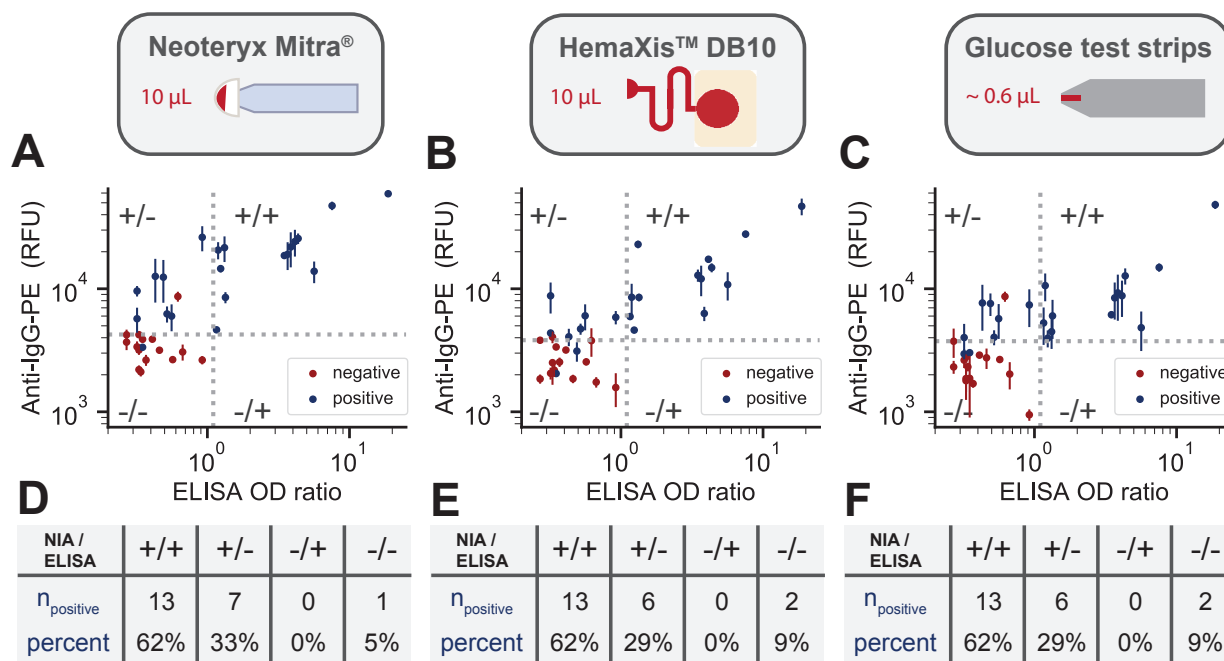


Figure 5: **Ultra-low volume patient sample collection and analysis.** (A-C) NIA anti-IgG-PE signal versus ELISA OD ratio for whole blood patient samples collected using each of the three sampling methods: Neoteryx Mitra®, DBS Systems SA HemaXis™ DB10, and glucose test strips. Data points are colored either blue or red corresponding to whether the samples were presumed positive or negative. The vertical dashed line represents the positive-negative cutoff for ELISA and the horizontal dashed line represents the chosen cutoff for the NIA measurements set equal to the 2nd highest negative measurement. Data points represent means  $\pm$ SD ( $n=4$ ). (D-F) Number of blue data points for each quadrant in plots A-C, respectively, along with the percentage of positive data points per quadrant.

185 collection methods. As a surrogate for capillary blood we used 36 EDTA-whole blood samples from 21 RT-  
 186 PCR confirmed COVID-19 patients and 15 presumed negative patients hospitalized for other reasons that  
 187 served as negative controls. We collected whole blood samples in Geneva followed by shipping via regular  
 188 mail to Lausanne for analysis. All positive samples are early seroconverts obtained within 14 days post  
 189 diagnosis, and thus even standard, large-volume serum samples are challenging to analyze (Fig. 2C). For  
 190 reference measurements we prepared plasma from EDTA-whole blood samples and performed S1 ELISA  
 191 assays on the same patient samples.

192 We directly compared results obtained by ELISA performed on standard large-volume serum samples  
 193 to NIA measurements performed on ultra-low volume dried whole blood samples collected with the three

194 collection methods and processed as described above (Fig. 5). ELISA detected SARS-CoV-2 specific  
195 antibodies in 62% of all COVID-19 patient samples and found no detectable antibodies in any of the 15  
196 presumed negative samples. For the three sampling methods we set the threshold between positive and  
197 negative calls to the intensity of the second highest negative sample. All three methods identified the same  
198 62% anti-SARS-CoV-2 IgG positive samples as the reference ELISA, but the Mitra<sup>®</sup> method was able to  
199 detect antibodies in 33% additional RT-PCR positive samples and the HemaXis<sup>™</sup> DB10 and glucose strip  
200 methods were able to detect an additional 29%. This proof of concept study demonstrates that ultra-volume  
201 whole blood samples can be collected and analyzed on the NIA platform. Surprisingly, even difficult to  
202 quantitate samples obtained within the first 14 days post onset of symptoms could be analyzed with this  
203 approach.

## 204 Discussion

205 We developed and validated a high-throughput nano-immunoassay device capable of analyzing 512-1024  
206 samples in parallel. Detecting the presence of SARS-CoV-2 anti-spike IgG antibodies with a 512 sample  
207 throughput per device the method achieved a specificity of 100% and a sensitivity of 98% based on the  
208 analysis of serum samples from 155 positive SARS-CoV-2 infected and 134 negative individuals, performing  
209 as well or better than standard ELISA (Fig. 6A). When analyzing 1024 samples per device the method  
210 achieved a sensitivity of 95%. In addition to generating accurate binary classification of samples, NIA is  
211 also capable of returning accurate antibody titers.

212 The method developed here is applicable to the large-scale characterization of serum samples collected  
213 as part of epidemiological studies, identify donors for plasma therapy, and vaccine trial support. A single  
214 researcher can achieve a throughput of 1-2 devices, or 512 - 1024 samples per day (analyzed in duplicate) in  
215 a small research laboratory not dedicated or equipped for high-throughput molecular diagnostics. Due to in-  
216 creases in efficiency, a small team of 3 can likely achieve a throughput of 6 devices or 3'072 samples per day  
217 (analyzed in duplicate). By comparison, the number of RT-PCR tests performed in all of Switzerland ranged  
218 from 6'000 to 18'000 tests per day between April and September 2020. Consumables, reagent consump-  
219 tion, and associated costs are negligible with NIA, which is an important consideration when compared to  
220 the high reagent cost of ELISAs and when considering potential reagent shortages that may be encountered  
221 during critical phases in a global pandemic.

222 To implement the method, laboratories require a commercially available contact microarrayer, and the

223 ability to fabricate masks, molds and PDMS microfluidic devices. Instruments required for photolitho-  
224 graphic fabrication of masks and molds are available at most major research universities, and mask fabrica-  
225 tion can be outsourced to service-based companies. PDMS microfluidic device fabrication can be conducted  
226 in a standard research laboratory with low-cost equipment: a spin-coater, 80°C oven, and stereo-microscope.  
227 To run the microfluidic devices, standard pressure regulators, pressure gauges, and manual or solenoid valves  
228 are used. Device readout is performed on a standard epi-fluorescence microscope equipped with an auto-  
229 mated stage.

230 Platform capabilities could be further expanded in the near term. We previously demonstrated that the  
231 platform can be used to perform multiplexed analysis, allowing 4 or more biomarkers to be tested for each  
232 sample [17, 24, 18]. This would allow the analysis of multiple antigens, cytokines, or inflammatory markers  
233 to provide insights into prior virus exposures and the response to infection. It should also be possible to  
234 detect IgA and IgM isotypes by using detection antibodies specific for these isotypes and to do so in a  
235 multiplexed format in which all 3 isotypes, IgG, IgA, and IgM are measured per sample. We also previously  
236 demonstrated that kinetic rate measurements can be performed in high-throughput with this method [25] and  
237 that digital ELISAs can be performed using the same technology in instances where lower limits of detection  
238 may be required [26, 11].

239 To enable large-scale studies we placed specific emphasis on the development of simple, low-cost, and  
240 ultra-low volume sample collection strategies and integration of these workflows with the nano-immunoassay  
241 platform. We characterized three blood sampling devices and tested all of them with patient samples. Two  
242 of these methods are commercially available devices: Mitra<sup>®</sup> from Neoteryx and HemaXis<sup>™</sup> DB10 from  
243 DBS System SA. We also explored the possibility of repurposing low-cost, and readily available blood glu-  
244 cose test strips for blood sample collection and shipment. The two commercial devices allow the collection  
245 of a minimal volume of 10  $\mu$ L whereas the blood glucose test strip collects as little as 0.6  $\mu$ L whole blood.  
246 Such small volumes allow untrained personnel to fingerprick and collect whole blood, eliminating the need  
247 for phlebotomists and the inconvenience of visiting a hospital or point of care location. The collected blood  
248 is allowed to dry on the devices, and we could show that these dried blood samples can be analyzed after 6  
249 days of storage at ambient temperatures eliminating the need for a cold chain.

250 The combination of a high-throughput, highly specific and sensitive nano-immunoassay, and the abil-  
251 ity to analyze minute volumes of dried blood samples has enormous potential for SARS-CoV-2 serology,  
252 epidemiological studies, vaccine trial and therapeutic development support. Further areas of use could be  
253 large-scale seroprevalence studies in low- and middle-income countries [28] without sufficient in-country

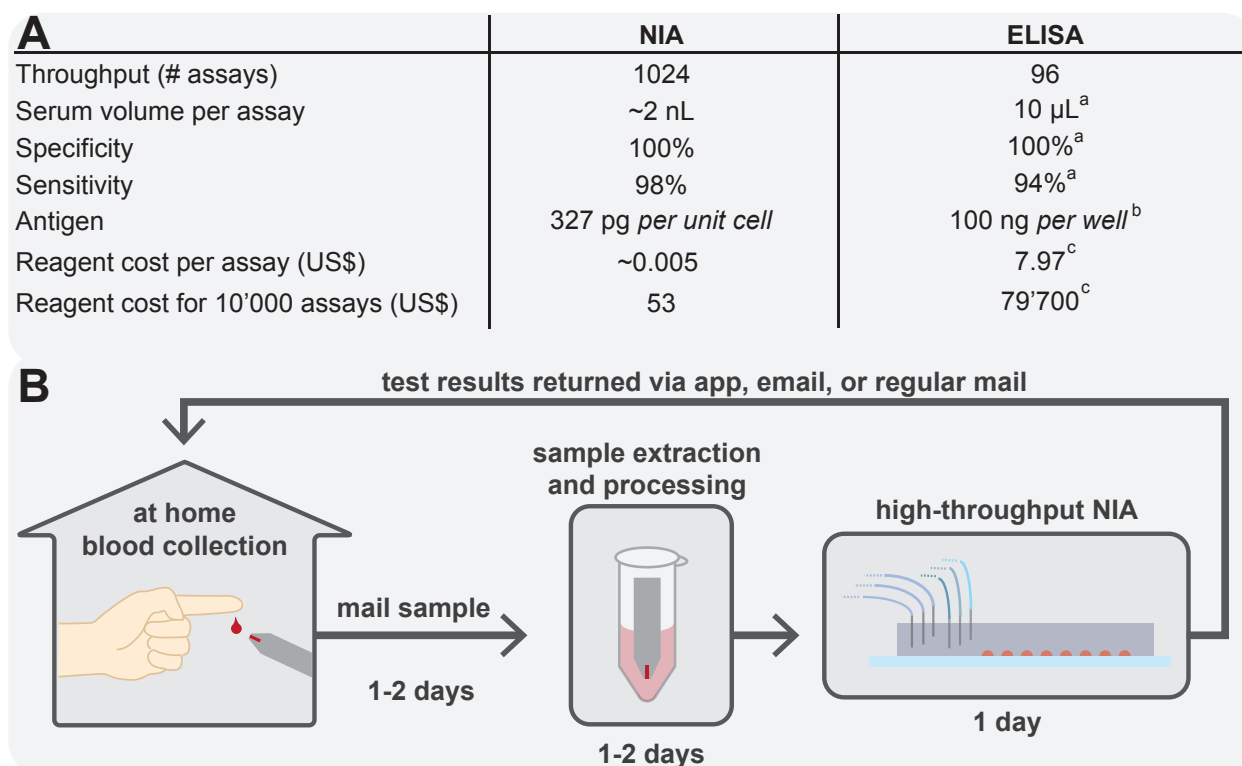


Figure 6: **NIA performance table and conceptual home-based sample collection and centralized NIA analysis.** (A) Comparison between the high-throughput NIA platform and standard ELISA. Sensitivity and specificity values are based on serum sample analysis for both NIA and ELISA. <sup>a</sup> based on EuroImmun ELISA kit (EI 2606-9601)[27], <sup>b</sup>[23], <sup>c</sup> price based on abcam ELISA kit (ab274342). (B) A NIA based diagnostic workflow that uses decentralized ultra-low volume whole blood sample collection, shipping via regular mail, and centralized sample processing and analysis on a high-throughput NIA platform. Test results are analyzed and interpreted and then reported back via mobile app, email, or regular mail.

254 laboratory capacity by sending specimens by international mail. Especially in the current SARS-CoV-2 pan-  
 255 demic, population-based seroprevalence studies could elucidate some urgent questions such as the impact  
 256 of COVID-19 in Africa [29].

257 New technology and method developments such as those reported here will make it possible to over-  
 258 come the current centralized molecular diagnostics paradigm, which is focused on hospitals and point of  
 259 care settings rather than on patients and individuals seeking simple, affordable, and convenient molecular  
 260 diagnostics. The need to visit a clinic is an inconvenience for everyone and can be an insurmountable ob-  
 261 stacle for many. The requirement for venipuncture blood collection, sample pre-treatment, and expensive



262 ELISAs prohibits broad testing and contributes to high health care costs. NIA makes it possible for individ-  
263 uals to purchase a simple blood sampling kit containing a lancet, a blood sampling device, and a return mail  
264 envelope, at a local pharmacy or supermarket (Fig. 6B). The kit can be used easily and conveniently in the  
265 privacy of one's own home, where a simple fingerprick is made and the blood collected by the device. The  
266 device with the collected blood can then be sent without special biosafety requirements by regular mail to  
267 a central laboratory which analyzes the blood sample for one or more biomarkers, interprets the data, and  
268 returns the test results to the individual via smart phone, email, or regular mail. Furthermore, each blood  
269 sample is sufficient to conduct many molecular diagnostic assays with NIA. The whole process from kit  
270 purchase to results could take less than a week, which is fast enough for a vast majority of tests that are  
271 not particularly time critical. Decentralized and simple sample collection coupled with centralized, next-  
272 generation high-performance molecular tests will broaden access to molecular diagnostics, and increase the  
273 use of testing. During a global pandemic, such technologies could enable the collection of critical epidemi-  
274 ological data, provide instrumental data for vaccine development, and provide information to individuals on  
275 their health status.

## 276 **Methods**

### 277 **Microfluidic chip fabrication**

278 The designs for the flow and control layer of the device were drawn with AutoCAD software and are avail-  
279 able for download ([lbnc.epfl.ch](http://lbnc.epfl.ch)), we then used standard photolithography to fabricate the molds for each  
280 layer. Three replicates of the design are fitted onto a 4 inch silicon wafer so that three devices can be made  
281 in a single fabrication process. SU-8 negative photoresist was used to create the control channel features  
282 (GM 1070, Gersteltec Sarl) with a height of 30  $\mu\text{m}$ , while AZ 10XT-60 positive photoresist (Microchemicals  
283 GmbH) was used to generate flow channel features with a height of 15  $\mu\text{m}$ . After development, the flow  
284 layer mold was annealed at 180°C in a convection oven for two hours to obtain rounded features. After-  
285 wards each of the wafers was treated with TMCS (trimethylchlorosilane) and coated with PDMS (Sylgard  
286 184, Dow Corning). For the control layer ~50 g of PDMS with an elastomer to crosslinker ratio of 5:1 was  
287 prepared, whereas for the flow layer a 20:1 ratio of elastomer to crosslinker was spin coated at 400 rpm to  
288 yield a height of ~50  $\mu\text{m}$ . Both PDMS coated wafers were then partially cured for 20 minutes at 80°C, after  
289 which devices from the control layer were cut out and the inlets for each control line were punched (OD =  
290 889  $\mu\text{m}$ ) using a precision manual-punching machine (Syneo, USA). Each control layer is then aligned onto

291 the flow layer by hand using a Nikon stereo microscope. The aligned devices were then placed at 80°C for  
292 90 minutes, allowing the two layers to bond together so that the entire device can then be cut and removed  
293 from the flow wafer. After that, the flow layer inlets were punched.

## 294 **Immunoassay reagents**

295 For our on-chip immunoassay we used biotinylated mouse anti-His antibodies (Qiagen, 34440) to immobi-  
296 lize His-tagged SARS-CoV-2 antigens on the surface of our assay chambers. The prefusion ectodomain of  
297 the SARS-CoV-2 spike glycoprotein (the construct was a generous gift from Prof. Jason McLellan, Uni-  
298 versity of Texas, Austin [30]) was transiently transfected into suspension-adapted HEK293 cells (Thermo  
299 Fisher) with PEI MAX (Transfection grade linear polyethylenimine hydrochloride, Polysciences) in Ex-  
300 cell293 medium. Incubation with agitation was performed at 37°C and 4.5% CO<sub>2</sub> for 5 days. The clarified  
301 supernatant was loaded onto Fastback Ni<sup>2+</sup> Advance resin column (Protein Ark) eluted with 500 mM imida-  
302 zole, pH 7.5 in PBS. For proof-of-concept experiments, chimeric anti-spike antibodies were purchased from  
303 Sino Biological (40150-D002, 40150-D003, 40150-D004, 40150-D005). We spiked the chimeric anti-spike  
304 antibodies into human serum (Sigma-Aldrich, H4522) and whole blood (ZenBio, SER-WB). For detecting  
305 human IgG, we used PE labeled goat anti-Human-IgG (Abcam, ab131612).

## 306 **Sample preparation**

### 307 **Serum**

308 Serum samples were collected from 155 RT-PCR confirmed COVID-19 patients and 134 negative control  
309 sera obtained in 2013/14 and 2018 before the start of the pandemic (including 50 children). All samples were  
310 collected according to the local ethical guidelines and ethical approval was waived by the ethics committee of  
311 the University Hospital of Geneva (HUG). We used days post onset of symptoms (dpos) according to patient  
312 history or days post diagnosis (dpd) in case dpos was unknown. All samples were stored at -20°C until  
313 analysis. In order to handle patient serum samples in a Biosafety Level 1 laboratory, patient serum samples  
314 were heat treated at 56°C for 30 minutes and Triton X-100 (Fisher Scientific) was added to the samples to a  
315 final concentration of 1%. In order to optimize spotting parameters and the on-chip immunoassay, proof-of-  
316 concept experiments involving human serum spiked with chimeric anti-spike antibodies were also carried  
317 out with the addition of Triton X-100. For dilution series experiments, patient serum samples were diluted  
318 in a PBS solution containing 2% BSA. Additionally, 10 μM fluorescein isothiocyanate(FITC)-dextran (10

319 kDa) was added as a tracer to each sample in order to assess whether similar volumes of serum samples  
320 were spotted (Fig. S9).

### 321 **Whole and dried blood**

322 Human Whole Blood - Frozen, 10ml was obtained from AMS Biotechnology (Europe). Anti-spike antibod-  
323 ies (Sino Biological) were added to whole blood to the desired concentration from a stock solution of 2  $\mu$ M.  
324 To simulate a fingerprick collection, 15-20  $\mu$ L of whole blood samples were pipetted on parafilm and then  
325 collected on the sampling device where 10  $\mu$ L were collected with HemaXis<sup>TM</sup> DB10 (DBS System SA) or  
326 Mitra<sup>®</sup> Clamshell (Neoteryx). The samples were dried and then stored in their original container without  
327 further protection. Samples were kept at room temperature for 1, 2 or 6 days, or in a 55°C oven for 1 day.  
328 The dried blood stored on HemaXis<sup>TM</sup> filter paper were cut using an 8 mm biopsy puncher and scalpel and  
329 the tip of the Mitra<sup>®</sup> devices were removed with tweezers. The samples were placed in a 96-well plate and  
330 filled with 200  $\mu$ L of cold extraction buffer (1xPBS, 1% BSA, 0,5% Tween20) [23] and incubated overnight  
331 at 4°C with 300 rpm agitation. Around 150  $\mu$ L per well of the supernatant was recovered and stored at -20°C  
332 until analysis. Alternatively, a small volume of blood (around 0.6  $\mu$ L) was collected with a Meditouch 2  
333 glucose test strip (Medisana), dried and stored in a box kept at room temperature for 1,2 or 6 days, or in a  
334 55°C oven for 1 day. Extraction was performed by placing the strip at the bottom of a 1,5 mL tube filled  
335 with 30  $\mu$ L of extraction buffer overnight at 4°C.

336 As a substitute for capillary blood taken from a fingerprick, we used leftover EDTA whole blood sam-  
337 ples drawn from hospitalised COVID-19 patients at different time points post diagnosis for routine clinical  
338 laboratory analysis. EDTA whole blood samples were stored at 4°C for a maximum of seven days before  
339 they were applied to the dried blood collection devices. 20  $\mu$ L of EDTA whole blood was pipetted on a  
340 parafilm sheet, and collected with a Mitra<sup>®</sup> device or glucose strip. For the HemaXis<sup>TM</sup> device, 10  $\mu$ L of  
341 whole blood was directly pipetted on the filter card. The samples were dried for 30 minutes and placed in  
342 a plastic bag with silica gel before shipping. The samples were extracted as described above 5 days after  
343 collection and shipping, microarray spotted on a glass slide on day 6 and the nano-immunoassay chip was  
344 run on day 7. To determine antibodies against SARS-CoV-2 S1 protein by Euroimmun S1 ELISA, EDTA  
345 whole blood samples were centrifuged for 5min at 1200x g at 4°C and 200  $\mu$ L of plasma were stored at  
346 4°C until analysis.

### 347 **SARS-CoV-2 serological assays**

348 Euroimmun S1 IgG ELISA (Euroimmun AG, Lübeck, Germany, # EI 2606-9601 G) was performed ac-  
349 cording to the manufacturers instructions and was run on a Dynex Agility (RUWAG Handels AG, Bettlach,  
350 Switzerland). OD ratios were calculated by dividing the OD450 of each sample by the OD450 of a calibrator  
351 that was run on each plate. Results equal or above OD ratio of 1.1 were considered positive. The LIAISON  
352 SARS-CoV-2 S1/S2 IgG ELISA was run on the LIAISONR XL analyzer, (Diasorin, Italy), the EDI Novel  
353 Coronavirus COVID-19 IgG ELISA (Epitope Diagnostics, USA) on the DSX analyzer (Dynex, Switzerland)  
354 and the Elecsys Anti-SARS-CoV-2 N (anti-N total antibodies) as well as the Elecsys Anti-SARS-CoV-2 S  
355 (anti-S1-RBD total antibodies) on the Cobas e801 analyzer (Roche Diagnostics, Switzerland) according to  
356 the manufacturers instructions.

### 357 **Microarray spotting**

358 25  $\mu\text{L}$  of each sample were loaded into a 384 microwell plate (ArrayIt, MMP384). An MP3 microarray  
359 printing pin (Arrayit) was used to spot the samples onto an epoxy-coated glass slide using a QArray2 mi-  
360 croarrayer (Genetix). The presence of Triton X-100 in the serum samples had a significant effect on the spot  
361 diameter. To account for this we increased the dimensions of the spotting chamber and set the inking and  
362 stamping time to 50 ms and 1 ms, respectively. In addition, it was critical that the ambient humidity was  
363 below  $\sim 42\%$ , otherwise the spots would become too large and merge together. After spotting, the PDMS  
364 chip was aligned on top of the sample spots using a stereo microscope and bonded over night at 40 °C.

### 365 **Running on-chip immunoassays**

366 Control lines were filled with PBS, attached to the chip and pressurized at 145 kPa. The NIA device is  
367 a low-complexity device, and can therefore be either regulated with simple manual 3 way toggle switch  
368 valves or computer controlled solenoid valves (only needed in order to make the entire on-chip workflow  
369 fully automated). Control and flow pressures are set by standard pressure regulators using a building air  
370 supply as the pressure source and monitored with two pressure gauges, respectively. Detailed descriptions  
371 of a standard MITOMI setup [31] and more sophisticated computerized microfluidic control setups for con-  
372 trolling complex multi-layer microfluidic devices have been previously published [32, 33]. While isolating  
373 the spotted sample with the neck valve closed, the lower half of the unit cells were patterned with BSA-  
374 biotin (Thermo Fisher, 29130) and neutrAvidin (Thermo Fisher, 3100). First BSA-biotin was flowed at a

375 concentration of 2 mg/mL for 20 minutes, then neutrAvidin was flowed at a concentration of 1 mg/mL for  
376 20 minutes. A flow pressure of 27-34 kPa was maintained for each of the flow steps. Afterwards the button  
377 valve was actuated and BSA-biotin was flowed for an additional 20 minutes. In between each of these steps  
378 a solution of 0.005% Tween 20 (Sigma, P1379) in PBS was flowed for 5 minutes to wash away any unbound  
379 material. After surface functionalization, a 1  $\mu\text{g}/\text{mL}$  solution of biotinylated anti-His antibody in 2% BSA in  
380 PBS was flowed for 20 minutes. Next a 6.7  $\mu\text{g}/\text{mL}$  solution of His-tagged SARS-CoV-2 spike protein in 2%  
381 BSA in PBS was flowed for 20 minutes. The spike protein solution contained 25% chicken serum (Sigma,  
382 C5405), which served to block the surface and reduce non-specific binding. Before each of these steps the  
383 solution was first flowed for 2 minutes with the button valves down, allowing the solution to flow evenly  
384 into the entire device. After flowing each solution for 20 minutes, a wash step was performed by flowing  
385 0.005% Tween PBS for 5 minutes with the button valves down. Once the spike protein was attached to the  
386 surface, the serum spots were re-solubilized by opening the neck valve and allowing 0.005% Tween PBS  
387 to flow into the spotting chamber while the outlet valve was closed. The neck valve was then closed and  
388 0.005% Tween PBS was flowed for 5 minutes to prevent cross-contamination of samples in neighboring unit  
389 cells. The sandwich valves were then closed and the neck valve was released to allow any antibodies present  
390 in the serum spot to diffuse into the assay chamber. After an incubation of 70 minutes the button valve  
391 was opened and a second incubation of 60 minutes was carried out, permitting any anti-spike antibodies  
392 to bind to the spike protein. Any unbound material could then be washed away by flowing 0.005% Tween  
393 PBS for 5 minutes with the button and neck valves closed. A 5.6  $\mu\text{g}/\text{mL}$  solution of anti-IgG-PE was then  
394 flowed for 2 minutes with the buttons down, then for 10 minutes with the buttons up. The buttons were then  
395 closed and any unbound detection antibody was washed away by flowing 0.005% Tween PBS for 5 minutes.  
396 Each unit cell was then imaged with an exposure time of 300 ms using a Nikon ECLIPSE Ti microscope  
397 equipped with a LED Fluorescent Excitation System, a Cy3 filter set, and a Hamamatsu ORCA-Flash4.0  
398 camera (C11440).

## 399 **Data analysis**

400 The detection antibody signal was quantified using a custom Python script. ROC analysis was performed  
401 using GraphPad Prism. Cutoff values for the NIA measurements were chosen by maximizing both the  
402 specificity and sensitivity values.  $EC_{50}$  values were determined by fitting the dilution series data (1:256 -  
403 1:8) for each sample to a saturation binding curve,  $y = \frac{B_{max}x}{x+EC_{50}}$ . For all samples  $B_{max}$  was set to 65000.

## 404 **Acknowledgments**

405 We would like to thank the Protein Production and Structure Core Facility team at EPFL, specifically Dr.  
406 David Hacker, Dr. Florence Pojer, Dr. Kelvin Lau, Laurence Durrer and Soraya Quinche for production  
407 and purification of Spike 2P in mammalian cells. We thank Neeraj Dhar and the Mckinney lab at EPFL for  
408 their help in sample inactivation in BSL-3. We thank Isabelle Arm-Vernez and Sabine Yerly for technical  
409 assistance as well as Barbara Lemaitre and Catia Machado Delgado for sample preparation. In addition,  
410 we thank Guiseppe Togni for running serological assays. We kindly thank DBS System SA for generously  
411 providing us with HemaXis™ DB10 devices. This work was supported by the European Research Council  
412 under the European Union's Horizon 2020 research and innovation program Grant 723106 (SJM), SNF  
413 Project grant 182019 (SJM), SNF NRP 78 Covid-19 grant 198412 (SJM, IE, and BM), EPFL (SJM) and a  
414 grant from the Private Foundation of the Geneva University Hospital (IE).

## 415 **Author contributions**

416 SJM, BM, and IE developed the project. PC, DOA, NV, LK provided resources and advice on experiments.  
417 ZS, GM, HMY, performed experiments. ZS, GM, HMY, IE, BM, SJM, designed experiments, analyzed  
418 data, and wrote the manuscript.

## 419 **Competing interests**

420 The authors declare no conflict of interest.

## 421 **References**

- 422 [1] Zhou, P. *et al.* A pneumonia outbreak associated with a new coronavirus of probable bat origin. *Nature*  
423 **579**, 270–273 (2020).
- 424 [2] Dong, E., Du, H. & Gardner, L. An interactive web-based dashboard to track COVID-19 in real time.  
425 *The Lancet Infectious Diseases* **20**, 533–534 (2020).
- 426 [3] Perez-Saez, J. *et al.* Serology-informed estimates of SARS-CoV-2 infection fatality risk in Geneva,  
427 Switzerland. *The Lancet Infectious Diseases* (2020).

- 428 [4] Krammer, F. & Simon, V. Serology assays to manage COVID-19. *Science* **368**, 1060–1061 (2020).
- 429 [5] Amanat, F. *et al.* A serological assay to detect SARS-CoV-2 seroconversion in humans. *Nature*  
430 *Medicine* **26**, 1033–1036 (2020).
- 431 [6] Stringhini, S. *et al.* Seroprevalence of anti-SARS-CoV-2 IgG antibodies in Geneva, Switzerland  
432 (SEROCoV-POP): a population-based study. *The Lancet* **396**, 313–319 (2020).
- 433 [7] Xu, X. *et al.* Seroprevalence of immunoglobulin M and G antibodies against SARS-CoV-2 in China.  
434 *Nature Medicine* **26**, 1193–1195 (2020).
- 435 [8] Gudbjartsson, D. F. *et al.* Humoral Immune Response to SARS-CoV-2 in Iceland. *New England*  
436 *Journal of Medicine* (2020).
- 437 [9] Pollán, M. *et al.* Prevalence of SARS-CoV-2 in Spain (ENE-COVID): a nationwide, population-based  
438 seroepidemiological study. *The Lancet* **396**, 535–544 (2020).
- 439 [10] Emmenegger, M. *et al.* Early peak and rapid decline of SARS-CoV-2 seroprevalence in a Swiss  
440 metropolitan region. *medRxiv* (2020).
- 441 [11] Norman, M. *et al.* Ultrasensitive high-resolution profiling of early seroconversion in patients with  
442 COVID-19. *Nature Biomedical Engineering* 1–8 (2020).
- 443 [12] Whitman, J. D. *et al.* Evaluation of SARS-CoV-2 serology assays reveals a range of test performance.  
444 *Nature Biotechnology* 1–10 (2020).
- 445 [13] Andrey, D. O. *et al.* Head-to-Head Accuracy Comparison of Three Commercial COVID-19 IgM/IgG  
446 Serology Rapid Tests. *Journal of Clinical Medicine* **9**, 2369 (2020).
- 447 [14] Rudolf, F. *et al.* Clinical Characterisation of Eleven Lateral Flow Assays for Detection of COVID-19  
448 Antibodies in a Population. *medRxiv* 2020.08.18.20177204 (2020).
- 449 [15] Maerkl, S. J. & Quake, S. R. A Systems Approach to Measuring the Binding Energy Landscapes of  
450 Transcription Factors. *Science* **315**, 233–237 (2007).
- 451 [16] Garcia-Cordero, J. L. & Maerkl, S. J. Mechanically Induced Trapping of Molecular Interactions and  
452 Its Applications. *Journal of Laboratory Automation* **21**, 356–367 (2016).

- 453 [17] Garcia-Cordero, J. L., Nembrini, C., Stano, A., Hubbell, J. A. & Maerkl, S. J. A high-throughput  
454 nanoimmunoassay chip applied to large-scale vaccine adjuvant screening. *Integrative Biology* **5**, 650–  
455 658 (2013).
- 456 [18] Garcia-Cordero, J. L. & Maerkl, S. J. A 1024-sample serum analyzer chip for cancer diagnostics. *Lab*  
457 *on a Chip* **14**, 2642–2650 (2014).
- 458 [19] Thorsen, T., Maerkl, S. J. & Quake, S. R. Microfluidic Large-Scale Integration. *Science* **298**, 580–584  
459 (2002).
- 460 [20] Remy, M. M. *et al.* Effective chemical virus inactivation of patient serum compatible with accurate  
461 serodiagnosis of infections. *Clinical Microbiology and Infection* **25**, 907.e7–907.e12 (2018).
- 462 [21] Fordyce, P. M. *et al.* De novo identification and biophysical characterization of transcription-factor  
463 binding sites with microfluidic affinity analysis. *Nature Biotechnology* **28**, 970–975 (2010).
- 464 [22] Thevis, M. *et al.* Can dried blood spots (DBS) contribute to conducting comprehensive SARS-CoV-2  
465 antibody tests? *Drug Testing and Analysis* **12**, 994–997 (2020).
- 466 [23] Klumpp-Thomas, C. *et al.* Standardization of enzyme-linked immunosorbent assays for serosurveys  
467 of the SARS-CoV-2 pandemic using clinical and at-home blood sampling. *medRxiv* (2020).
- 468 [24] Garcia-Cordero, J. L. & Maerkl, S. J. Multiplexed surface micropatterning of proteins with a pressure-  
469 modulated microfluidic button-membrane. *Chemical Communications* **49**, 1264–1266 (2013).
- 470 [25] Geertz, M., Shore, D. & Maerkl, S. J. Massively parallel measurements of molecular interaction  
471 kinetics on a microfluidic platform. *Proceedings of the National Academy of Sciences* **109**, 16540–  
472 16545 (2012).
- 473 [26] Piraino, F., Volpetti, F., Watson, C. & Maerkl, S. J. A Digital–Analog Microfluidic Platform for Patient-  
474 Centric Multiplexed Biomarker Diagnostics of Ultralow Volume Samples. *ACS Nano* **10**, 1699–1710  
475 (2016).
- 476 [27] Meyer, B. *et al.* Validation of a commercially available SARS-CoV-2 serological immunoassay. *Clin-*  
477 *ical Microbiology and Infection* **26**, 1386–1394 (2020).



- 478 [28] Alvim, R. G. F. *et al.* An affordable anti-SARS-COV-2 spike protein ELISA test for early detection  
479 of IgG seroconversion suited for large-scale surveillance studies in low-income countries. *medRxiv*  
480 (2020).
- 481 [29] Chibwana, M. G. *et al.* High SARS-CoV-2 seroprevalence in Health Care Workers but relatively low  
482 numbers of deaths in urban Malawi. *medRxiv* (2020).
- 483 [30] Wrapp, D. *et al.* Cryo-EM structure of the 2019-nCoV spike in the prefusion conformation. *Science*  
484 **367**, 1260–1263 (2020).
- 485 [31] Rockel, S., Geertz, M. & Maerkl, S. J. MITOMI: A Microfluidic Platform for In Vitro Characterization  
486 of Transcription Factor–DNA Interaction. *Methods in Molecular Biology* **786**, 97–114 (2011).
- 487 [32] White, J. A. & Streets, A. M. Controller for microfluidic large-scale integration. *HardwareX* **3**, 135–  
488 145 (2017).
- 489 [33] Brower, K. *et al.* An Open-Source, Programmable Pneumatic Setup for Operation and Automated  
490 Control of Single and Multi-Layer Microfluidic Devices. *HardwareX* **1** – 37 (2017).

## Supplementary Figures

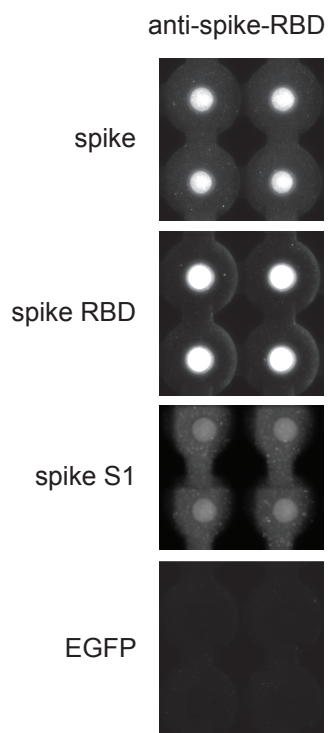


Figure S1: **Evaluation of SARS-CoV-2 antigens.** NIA images showing anti-IgG-PE signals obtained when spike, RBD and S1 antigens in combination with an anti-S1 primary antibody were tested. EGFP served as a negative control.

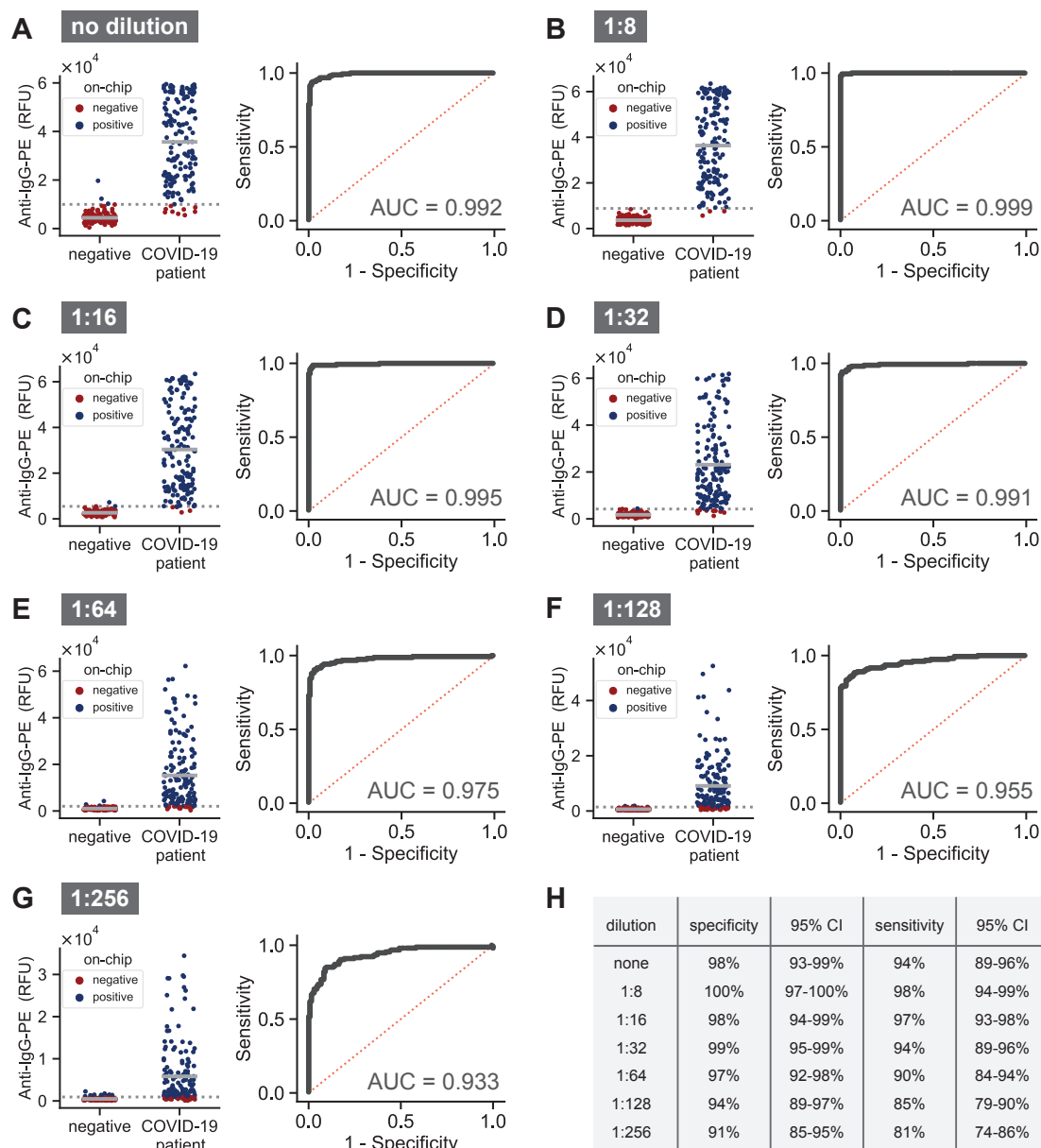


Figure S2: NIA measurements for a range of sample dilutions. (A-G) NIA measurements for different dilutions of patient serum samples categorized according to whether the sample was pre-pandemic negative or from COVID-19 patients. Data points represent mean values ( $n = 3$ ). Corresponding ROC curves are shown to the right of the plotted data. (H) Specificity and sensitivity values calculated for each dilution according to the dashed cutoff line shown in plots A-G.

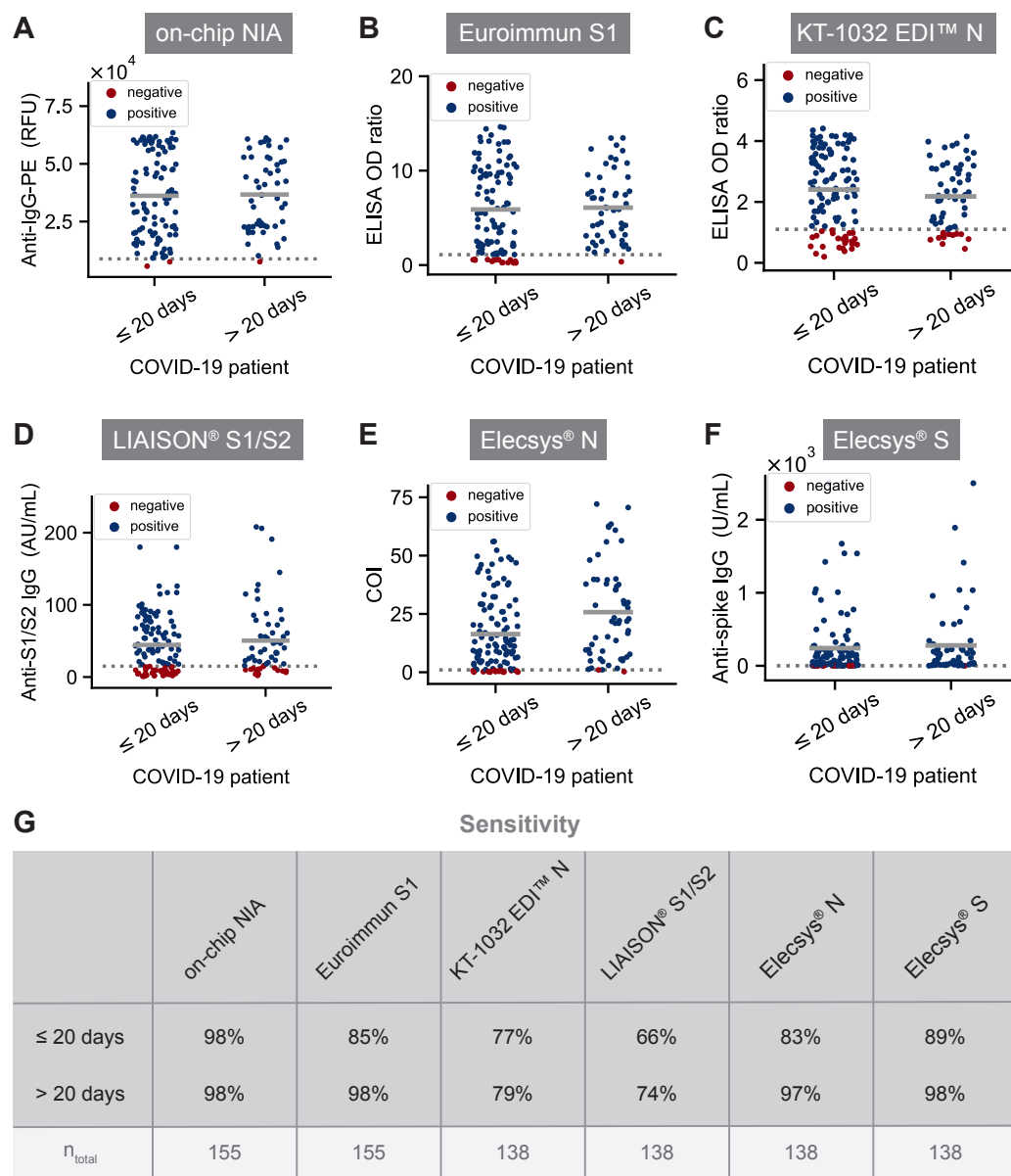


Figure S3: **Comparison of NIA with commercial assays.** (A-F) Levels of anti-SARS-CoV-2 IgG antibodies present in serum collected from COVID-19 patients ≤20 days or >20 days post onset. (G) Sensitivity values calculated for each assay according to the dashed cutoff line shown in plots A-F. The manufacturer recommended cutoffs were used for the commercial assays. The total number of patient serum samples tested for each assay is listed below the sensitivity values.

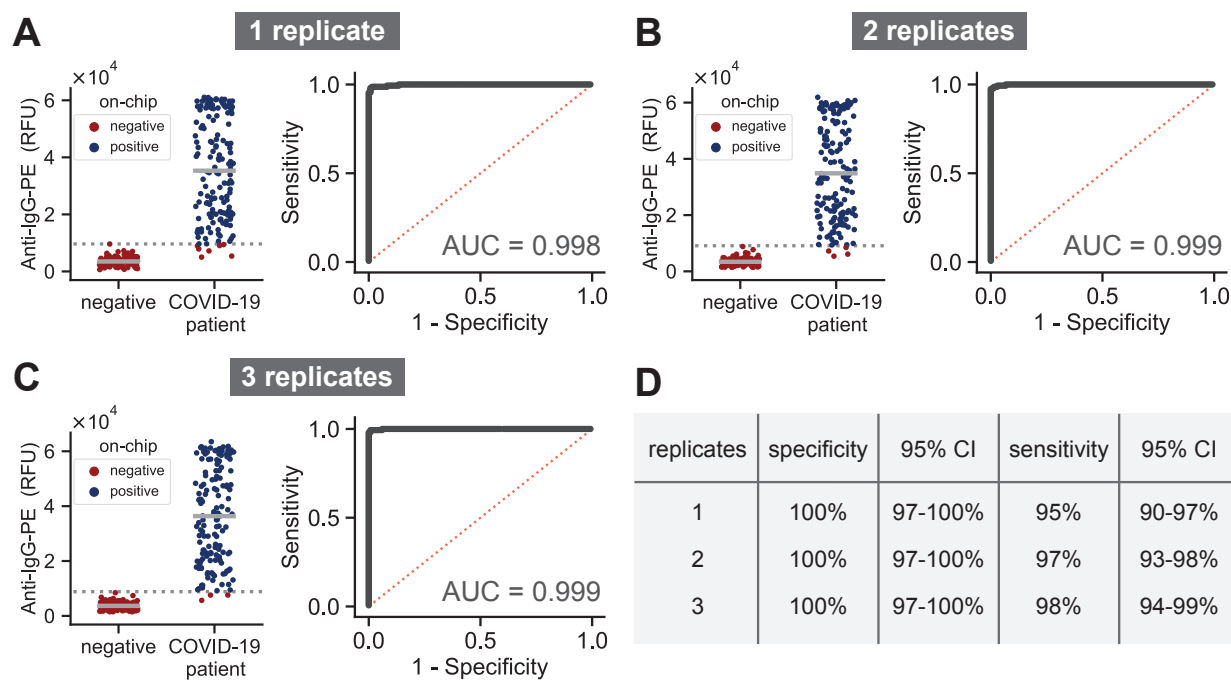


Figure S4: **NIA replicates.** (A-C) Mean anti-IgG-PE signal for one, two or three on-chip replicates shown for a 1:8 serum dilution, along with the corresponding ROC curves. (D) Specificity and sensitivity values calculated according number of on-chip replicates and based on the dashed cutoff line shown in plots A-C.

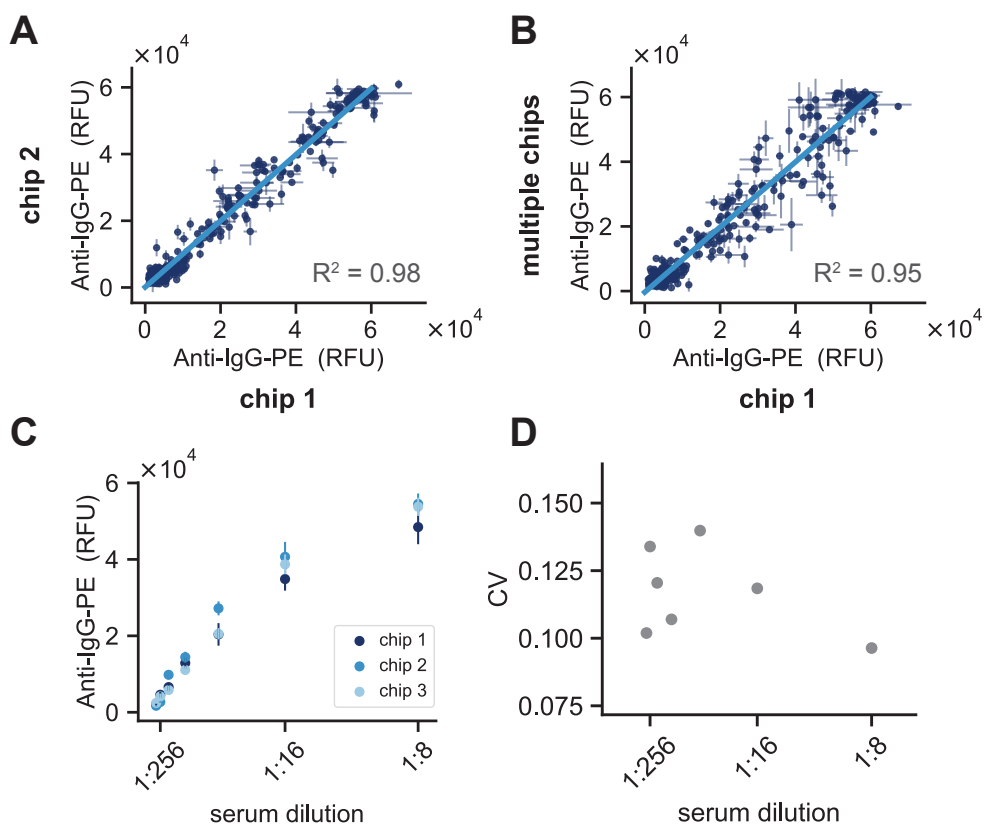


Figure S5: **Device-to-device variation.** (A) Correlation of anti-IgG-PE signals obtained from two separate chips that were prepared using the same 1:8 serum sample dilutions. (B) Anti-IgG-PE measurements collected from a total of 6 chips versus measurements for the same samples collected on a single chip. Sample dilutions were prepared separately for each of the chips. (C) NIA measurements for a reference serum dilution series measured on three separate chips. (D) Coefficient of variation calculated for the three measurements of each reference serum dilution.

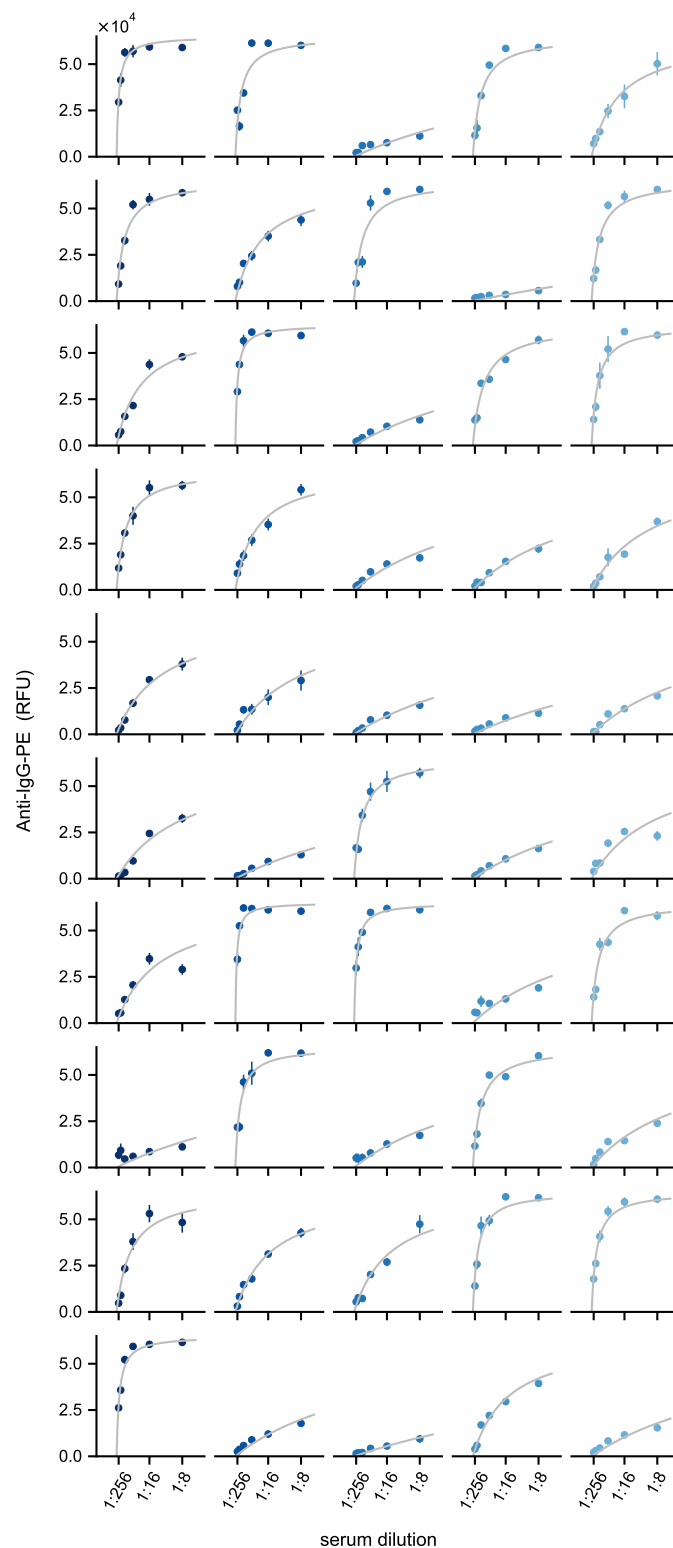


Figure S6: **Complete serum dilution data.** Data points are colored blue or red corresponding to dilutions from negative or positive patient serum samples, respectively.

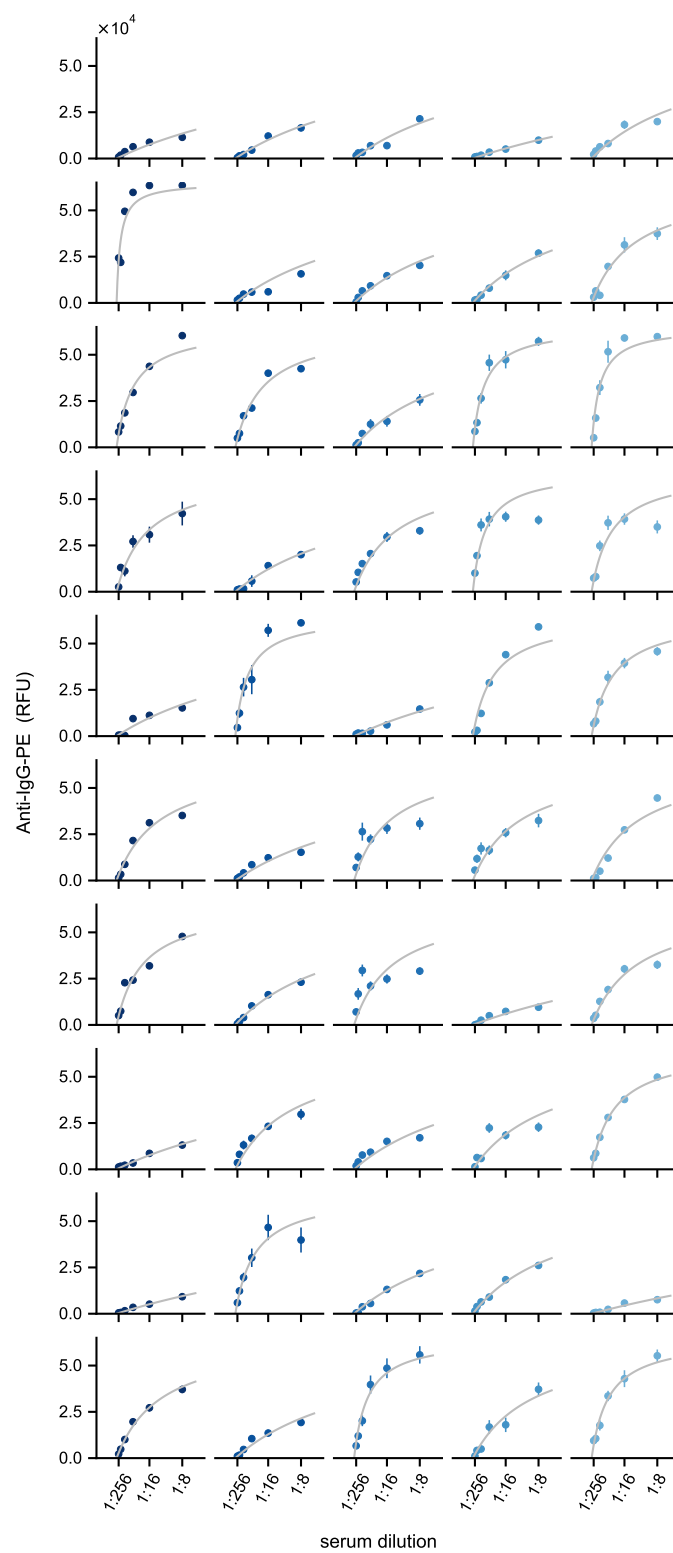


Figure S6: Complete serum dilution data.



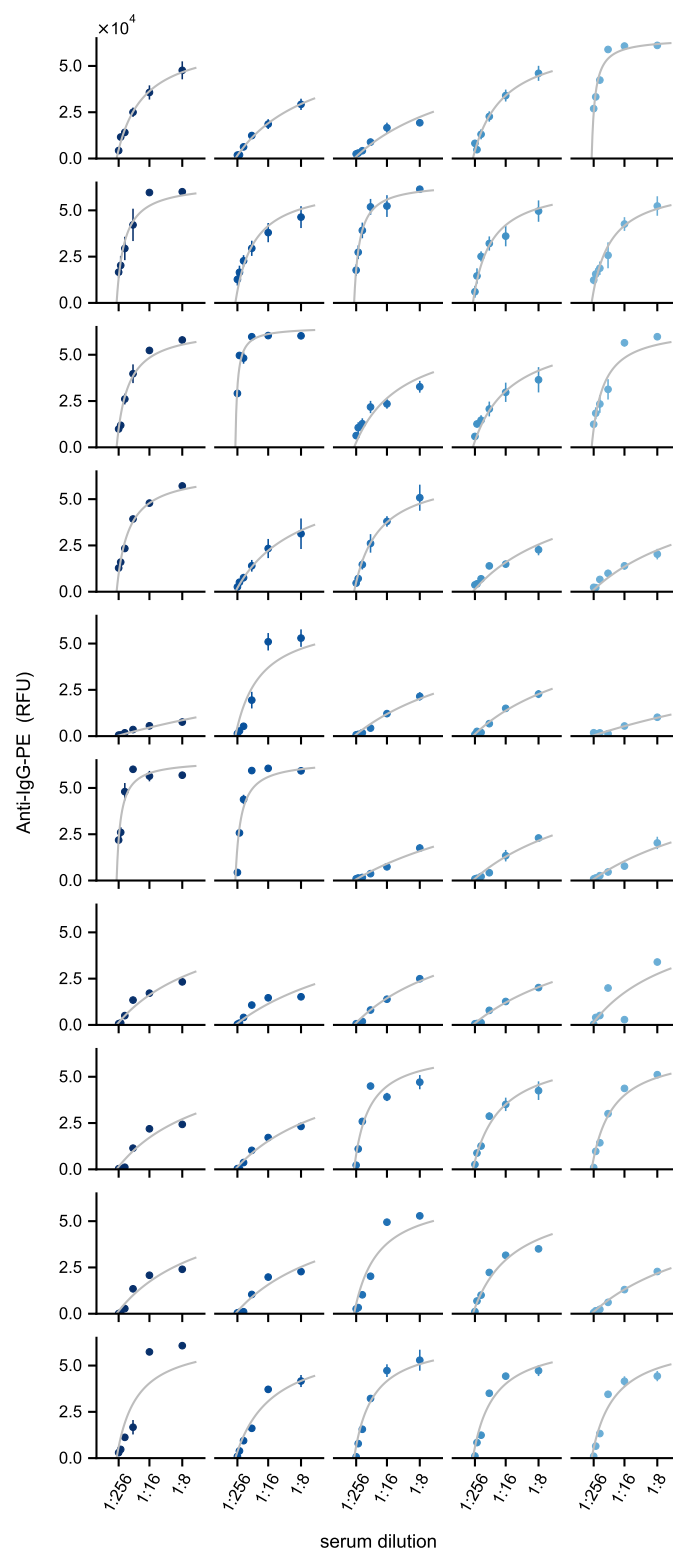


Figure S6: Complete serum dilution data.

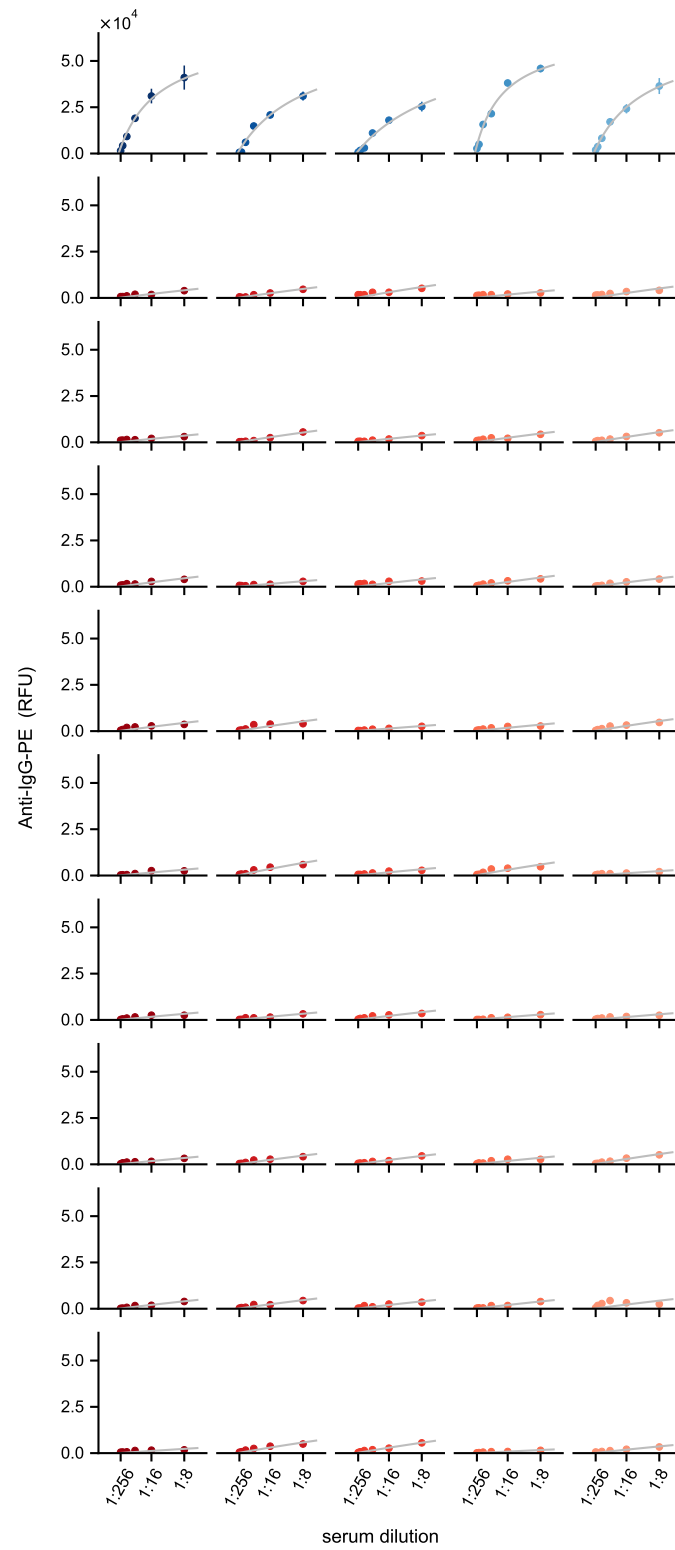


Figure S6: Complete serum dilution data.

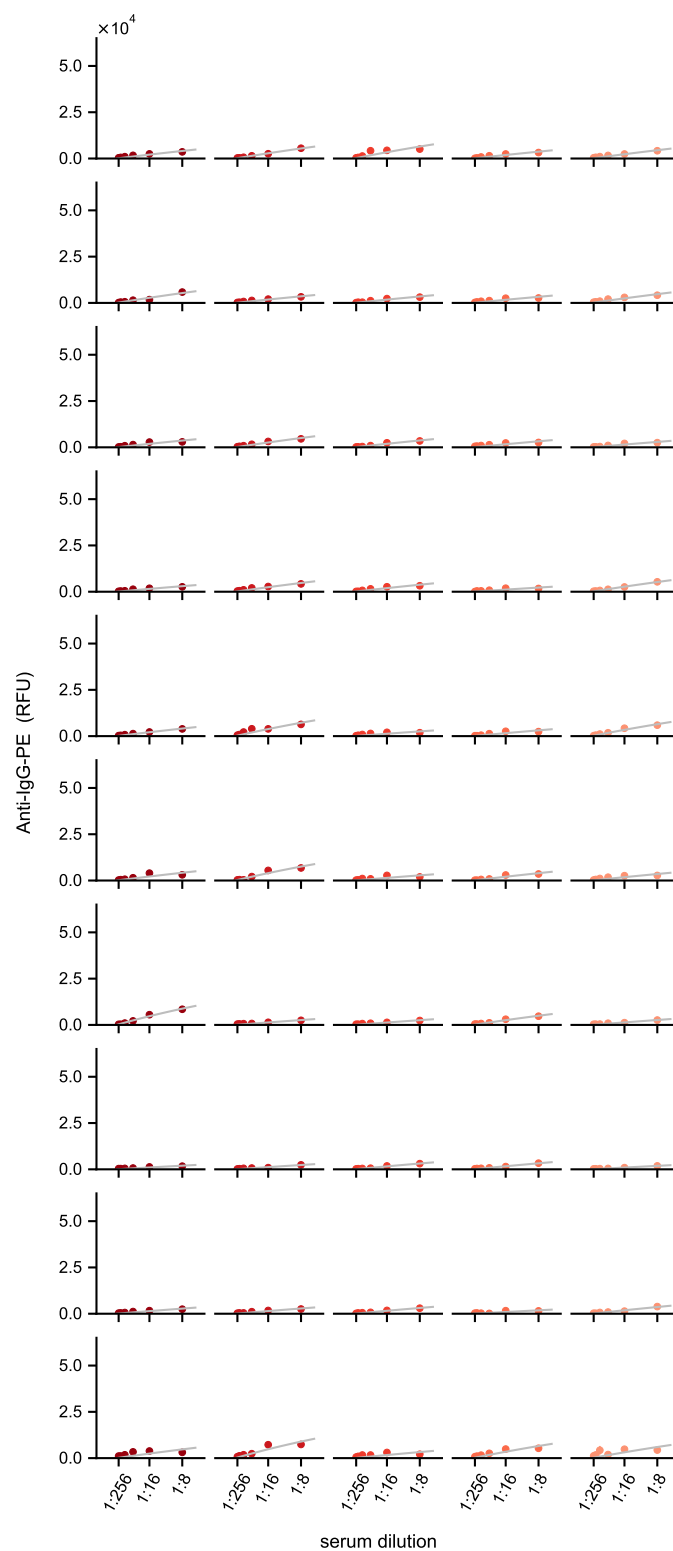


Figure S6: Complete serum dilution data.

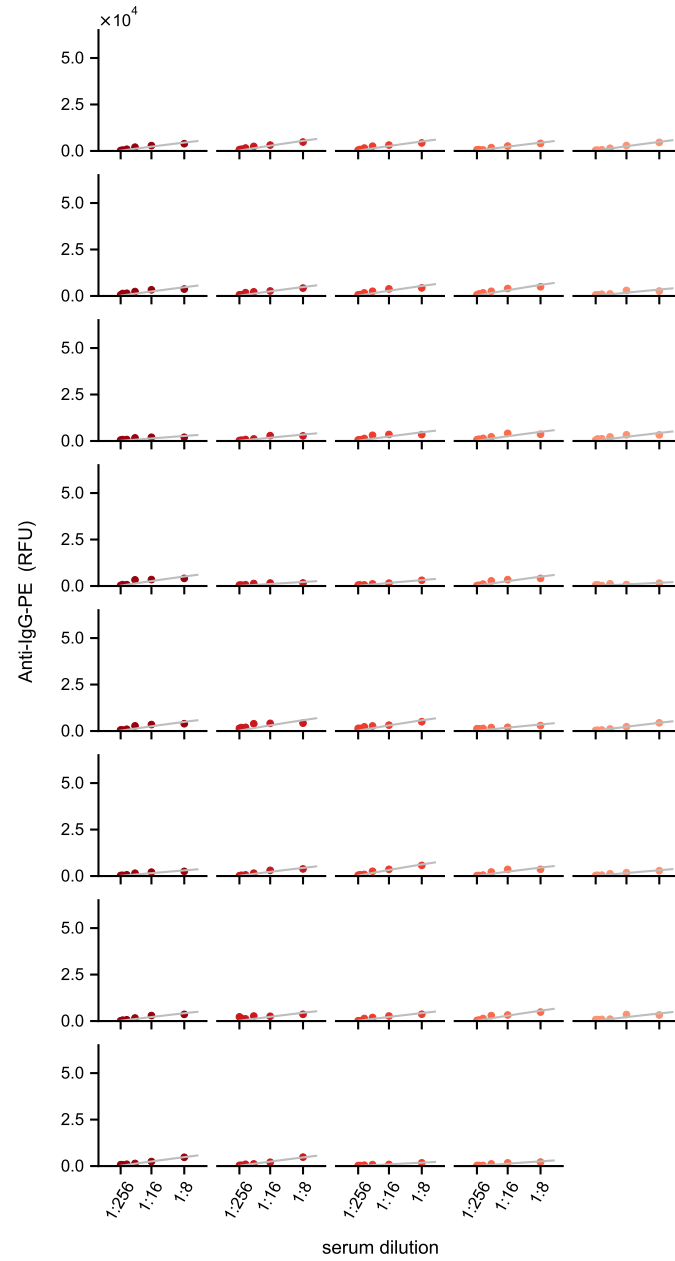


Figure S6: Complete serum dilution data.

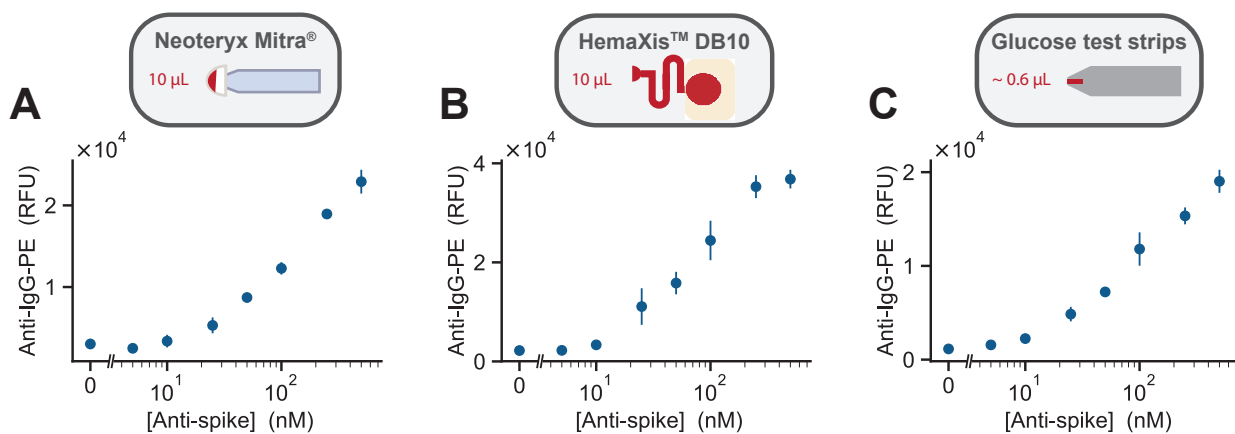
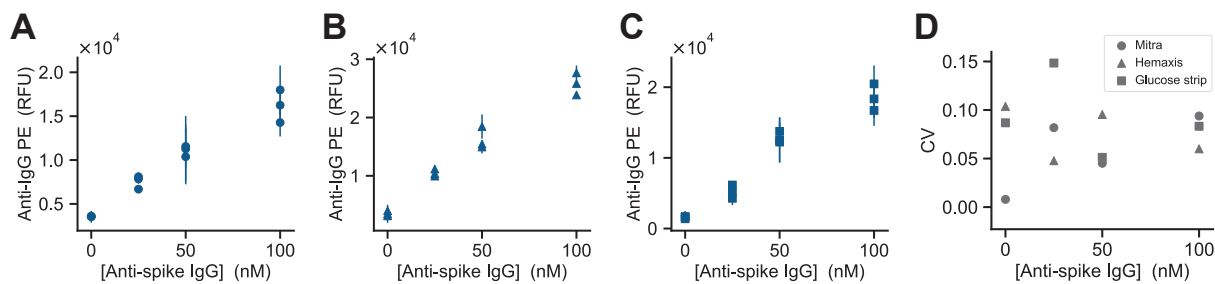


Figure S7: **Detection of anti-spike IgG in whole blood.** (A-C) Non-normalized on-chip anti-IgG-PE signal versus the concentration of anti-spike-IgG in whole blood sampled using each of the three methods: Mitra®, HemaXis™ DB10, and glucose test strips (shown in this order from left to right).



**Figure S8: Technical replicates for ultra-low volume whole blood sampling methods.** (A-C) On-chip anti-IgG-PE signal versus the concentration of anti-spike-IgG in whole blood for three technical replicates sampled using each of the three methods: Mitra<sup>®</sup>, HemaXis<sup>™</sup> DB10, and glucose test strips (shown in this order from left to right). (D) Coefficient of variation versus the concentration of anti-spike-IgG for each blood sampling method.

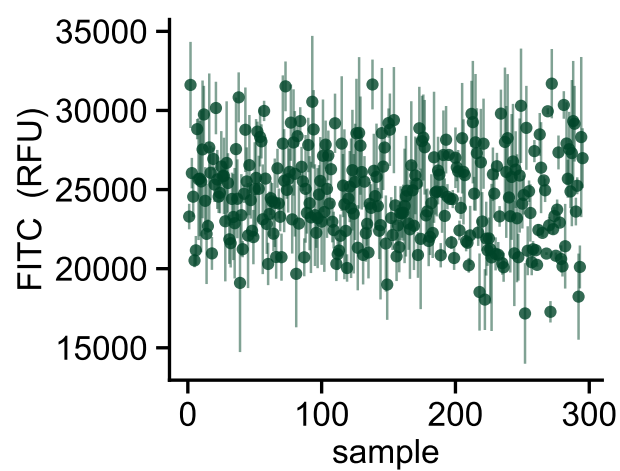


Figure S9: **FITC spotting tracer.** FITC-dextran (10 kDa) signal for each serum sample (1:8 dilution). Images were acquired in the spotting chamber after the sample had been resolubilized.